EXHIBIT V

PART 19

and

$$T_D = (CH)_{EPP+PPE} + \gamma\gamma + \gamma\delta^+ + \delta^+\delta^+ \quad (37)$$

$$= k(2EEE + EPP+PPE + PEEP + (1/2)[PEEE+EEEP]) \quad (38)$$

$$= k(2EEE + EPP+PPE + 1/2[PEE+EEP]) \quad (39)$$

Equation (39) expresses Region "D" in terms of triads only. It can still be expressed through tetrads by expanding the triads in Eq. (38) by utilizing the necessary triad-tetrad relationships of Table 1. The same is also true for Regions "C," "E," "G," and "H."

Region "E"

Range: 28–29.5 ppm
Contributing carbons: $(Methine)_{PPP}$
Observed *n*-ads: PPP

$$T_E = k(PPP) \quad (40)$$

Region "F"

Range: 27–28 ppm
Contributing carbons: $\beta\delta^+$
Observed *n*-ads: EPEE+EEPE, PPEE+EEPP

$$T_F = k[(EPEE+EEPE) + (PPEE+EEPP)] \quad (41)$$

$$= k(PEE+EEP) \quad (42)$$

Region "G"

Range: 24–25 ppm
Contributing carbons: $\beta\beta$
Observed *n*-ads: PPEPP, PPEPE+EPEPP, EPEPE

$$T_G = k(PPEPP + PPEPE+EPEPP + EPEPE) \quad (43)$$

$$= k(PEP) \quad (44)$$

Region "H"

Range: 19–22 ppm
Contributing carbons: Methyl
Observed *n*-ads: P

$$T_H = k(P) \quad (45)$$

$$= k(EPE + EPP+PPE + PPP) \quad (46)$$

The above eight equations, summarized in Table 11, are available to extract six triad concentrations. It should be noted that the above equations correctly sum to $k(3P + 2E)$ after invoking the appropriate necessary relationships. An overdetermination of the triad distribution is a desirable result from a quantitative viewpoint because it would allow the internal consistency of the ^{13}C-NMR data to be tested. Whether or not this can be done depends on the accuracy and dependability of the measurements from each NMR region. Accuracy should never be sacrificed and each E/P copolymer presents a different case. The level of stereochemical regularity is related to the choice of catalyst system and reactor conditions, line widths are affected by molecular weights, and the extent of overlap will often depend upon a particular E/P ratio. The final analytical method will, therefore, depend upon a number of factors. An illustration of how the final choice is made is given through the following example. Table 11 contains intensity data from each of eight spectral regions, as measured by digital integration, on the copolymer shown in Fig. 1. If all the regions

TABLE 11

Triad Equations and Intensities as Measured by Digital Integration of Regions A through H of an Ethylene–Propylene Copolymer in Fig. 1

$T_A = k(PPP + (1/2)[PPE+EEP])$	= 108.1
$T_B = k(PEP + (1/2)[PEE+EEP] + EPE + (1/2)[PPE+EPP])$	= 75.6
$T_C = k(EPE)$	= 18.2
$T_D = k(2EEE + [PPE+EPP] + (1/2)[PEE+EEP])$	= 96.8
$T_E = k(PPP)$	= 85.2
$T_F = k(PEE+EEP)$	= 31.2
$T_G = k(PEP)$	= 25.1
$T_H = k(PPP + [PPE+EPP] + EPE)$	= 147.5

were equally well-resolved and measured with the same degree of accuracy, a least-squares analysis could be employed to obtain the final triad concentrations. A better approach is to examine the data for systematic errors, which can be eliminated from the final result. An inspection of the triad equations in Table 11 shows that k(PPE+EPP) can be determined in five different ways:

$$k(PPE+EPP) = 2T_A - 2T_E = 45.8 \quad (47)$$

$$= T_B - 2T_C = 39.2 \quad (48)$$

$$= T_H - T_E - T_C = 44.1 \quad (49)$$

$$= 2T_G + T_F - 2T_C = 45.0 \quad (50)$$

$$= 2T_H - 2T_C - 2T_A = 42.4 \quad (51)$$

The average value for k(PPE+EPP) is 43.4. Good agreement is shown among the results for Eqs. (47), (49), and (50). Equation (48) gives a low result which displays the largest deviation from the average. A close examination of the ethylene–propylene copolymer spectrum in Fig. 1 reveals that the recorder trace does not quite return to the baseline between Regions D, E, and F. Under such circumstances, it is possible that equations containing these terms could yield high results. Therefore, Eqs. (47), (49), and (50), although in excellent agreement, could actually contain a systematic error. This possibility could be avoided by combining the data from Regions D, E, and F into one region, T_{DEF}, given below:

$$T_{DEF} = k(2EEE + [PPE+EPP] + (3/2)[PEE+EEP] + PPP) \quad (52)$$

Only Eqs. (48) and (51), which are in fairly good agreement, remain for the determination of k(PPE+EPP). These are averaged and the complete set of triad equations are calculated from the remaining data regions and T_{DEF}. The following results are obtained:

$$k(EEE) = (1/2)(T_{DEF} + T_A + T_C + 3T_G - T_B - 2T_H) = 22.1 \quad (53)$$

$$k(PEE+EEP) = T_H + (1/2)T_B - T_A - 2T_G = 27.0 \quad (54)$$

$$k(PEP) = T_G = 25.1 \quad (55)$$

$$k(EPE) = T_C = 18.2 \quad (56)$$

$$k(EPP+PPE) = (1/2)(2T_H + T_B - 2T_A - 4T_C) = 40.8 \quad (57)$$

$$k(PPP) = (1/2)(3T_A + 2T_C - (1/2)T_B - T_H) = 87.7 \quad (58)$$

The NMR constant, k, is eliminated from the above equations through normalization to yield the triad distribution:

(EEE) = 0.100

(PEE+EEP) = 0.122 (E) = 0.336

(PEP) = 0.114

(EPE) = 0.082

(EPP+PPE) = 0.185 (P) = 0.664

(PPP) = 0.397

The average sequence lengths are

$$n_E = \frac{(EEE) + (PEE+EEP) + (PEP)}{(PEP) + (1/2)(PEE+EEP)} = 1.9 \quad (59)$$

$$n_P = \frac{(PPP) + (PPE+EPP) + (EPE)}{(EPE) + (1/2)(EPP+PPE)} = 3.8 \quad (60)$$

and the sequence numbers are given by:

$$\text{Sequence number} = (100)[(PEP) + (1/2)(PEE+EEP)] = 17.5 \quad (61)$$

$$= (100)[(EPE) + (1/2)(EPP+PPE)] = 17.5 \quad (62)$$

Equations (61) and (62) permit an internal consistency check of the quantitative NMR data because the sequence number can be determined independently from either the E-centered or P-centered triads. The run number for this ethylene–propylene copolymer is 35, which means that there is a switch from ethylene to propylene and propylene to ethylene a total of 35 times per 100 repeat units. Prior to normalization, the sum of the NMR triad areas (Eqs. 53–58) lead to the "total *n*-ad intensity," which can be used to obtain normalized values for any of the directly measured tetrads or pentads. A partial tetrad or pentad set is useful when determining the conformity of the copolymer sequence distribution to a particular statistical model [61].

One way to check the validity for combining equations D through F is to redetermine the triad distribution using the average PPE+EPP from Eqs. (47)–(51). The EEE triad is now given by

$$k(EEE) = (1/2)T_D - (1/4)T_F - (1/2)k[PPE+EPP] \qquad (63)$$

and the following triad intensities are obtained:

$$k(EEE) = 18.9$$
$$k(PEE+EEP) = 31.2$$
$$k(PEP) = 25.1$$
$$k(EPE) = 18.2$$
$$k(PPE+EPP) = 42.2$$
$$k(PPP) = 85.2$$

Normalization gives the triad distribution:

$$(EEE) = 0.085$$
$$(PEE+EEP) = 0.141 \quad (E) = 0.339$$
$$(PEP) = 0.113$$
$$(EPE) = 0.082$$
$$(PPE+EPP) = 0.195 \quad (P) = 0.661$$
$$(PPP) = 0.384$$

A comparison with the initially determined triad distribution reveals that the E,P monad distributions are in good agreement while differences exist among the values obtained for the various triads. This is precisely the result expected if there is an overlap error in the triad determination. The monad distribution utilizes the necessary relationships which combine the contributing intensities, thus removing the overlap error. The original triad distribution combining D, E, and F probably gives the more accurate result. The sequence numbers also support the initial approach because their internal consistency, although not bad, is not so close as in the first approach:

$$\text{Sequence number} = (100)[(PEP) + (1/2)(PEE+EEP)] = 18.4$$
$$= (100)[(EPE) + (1/2)(EPP+PPE)] = 18.0$$

The average sequence lengths from the second method are

$$n_E = 1.8$$
$$n_P = 3.7$$

It is somewhat gratifying that the second method did not lead to serious errors, but there is also little doubt that the initial method gives the better result when Regions D, E, and F are combined. In general, specific tests for internal consistency can be developed utilizing the appropriate necessary relationships for each copolymer being analyzed. Care in the selection of regions for an analytical method can eliminate errors from overlap. Again, the use of NMR spectral regions eliminates the need for making many pentad and higher order *n*-ad assignments for closely spaced resonances from sequences differing only by chirality or because of branches located three to five carbons away. Such an approach leads to improved accuracy and increasing confidence in the determinations of triad distributions, sequence numbers, and average sequence lengths.

The groundwork has now been laid for similar developments in ^{13}C-NMR analyses of ethylene–1-butene, ethylene–1-hexene, and ethylene–1-octene copolymers. These treatments will not be discussed in such rigorous detail as was the case for the ethylene–propylene copolymer analyses, but some additional concepts will be introduced, as needed, along with the method

development. Certainly, trends in ^{13}C-NMR assignments will be noted and comparison made where appropriate.

VI. ETHYLENE–1-BUTENE COPOLYMERS

Ethylene–1-butene copolymers are one of the three important commercial linear medium- and low-density polyethylenes. The others are ethylene–1-hexene and ethylene–1-octene copolymers. The 1-butene comonomer has both advantages and disadvantages when compared to 1-hexene and 1-octene comonomers in commercial applications. It is readily available at a relatively low cost. The 1-butene comonomer has physical characteristics that make it ideally suited for gas-phase polymerizations. As is the case for the other 1-olefin copolymers, ethylene–1-butene copolymers meeting precise density and processing requirements can be prepared through control of the 1-butene incorporation [62]. The amount of incorporated 1-butene required to achieve a density level of approximately 0.92 g/cm^3 is usually in a range of 4 to 6 mol%, which is a slightly higher level than required for 0.92-g/cm^3 density in the corresponding 1-hexene and 1-octene copolymers. The 1-butene comonomer has a greater tendency to form 1-butene contiguous sequences, thus a higher incorporation is required to achieve the desired density level [15].

A ^{13}C-NMR spectrum at 50.3 MHz of a typical linear low-density ethylene–1-butene copolymer is reproduced in Fig. 8. A complete listing of chemical shift assignments, gathered from eight reference systems [15], is given in Table 12. The introduction of a 1-butene unit among contiguous ethylene repeat units leads to the presence of an ethyl branch on the polymer backbone. Contiguous 1-butene sequences lead to 1,3-diethyl and 1,3,5-triethyl branches, etc. As is clear from the spectrum in Fig. 8, a 0.92 density ethylene–1-butene copolymer has very few contiguous 1-butene sequences.

Model homopolymers and copolymers are also required to establish chemical shift assignments in the ^{13}C-NMR spectra of ethylene–1-butene copolymers. One very good model system for this purpose is a hydrogenated polybutadiene, where hydrogenation of 1,2-butadiene sequences produces ethyl branches analogous to ethylene–1-butene copolymers. The hydrogenated polybutadienes [63, 64] allow assignments for $\alpha\delta^+$ resonances to be determined independently of the various $\alpha\gamma$ resonances

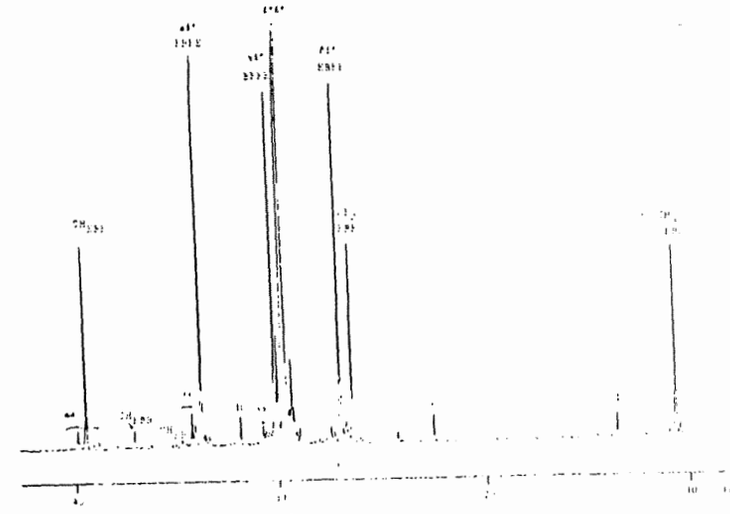


FIG. 8. 50.3 MHz carbon-13 NMR spectrum of an ethylene 1-butene copolymer at 125°C in 1,2,4-trichlorobenzene.

from EBEBE, EBEBB, and BBEBB. A sequence analogous to "BEB" is structurally impossible in hydrogenated polybutadienes, but the remaining structural sequences in hydrogenated polybutadienes are present in ethylene–1-butene copolymers. The chemical shift assignments are, therefore, uncomplicated by the presence of the various $\alpha\gamma$ and $\gamma\delta$ sequences. A 50.3-MHz ^{13}C-NMR spectrum of a hydrogenated polybutadiene containing 70 ethyl branches per 1000 total carbon atoms is reproduced in Fig. 9.

Ethylene–1-butene copolymers with increasing 1-butene contents are also useful model copolymers for establishing ^{13}C-NMR chemical shift assignments. A copolymer containing only 2.0 mol% 1-butene was useful for making ^{13}C-NMR chemical shift assignments associated with the EBE, EBEE+EEBE, EEEB+BEEE, EBEB+BEBE, and EBEBE sequences. The chemical

TABLE 12

Carbon-13 NMR Chemical Shift Assignments at 50.3 MHz for Ethylene–1-Butene Copolymers Containing Principally Isotactic 1-Butene Sequences and No Inverted 1-Butene Repeat Units. The Samples Were Prepared at 10% by Weight in 1,2,4-Trichlorobenzene (TCB) with Perdeuterobenzene Added and at 15% by Weight in Tetrachloroethane-d_2 (TCE-d_2). The Spectra Were Obtained at 125 ± 1°C. The $\delta^+\delta^+$ Peak Is Set at 29.98 ppm with Respect to an Internal Tetramethylsilane Standard

Chemical shift ppm, TMS		Carbon assignment	Sequence assignment
TCB	TCE-d_2		
40.20	40.3–40.4	αα	BBBB (mmm)
39.61	39.79	Methine	EBE
39.56	39.27	αα	BBBE+EBBB (mm)
39.28		αα	EBBE (r)[a]
38.98		αα	EBBE (m)
37.24	37.43	Methine	EBB+BBE (m)
34.98	35.1–35.2	Methine	BBB
34.81		αγ	BBEB+BEBB (mm)
34.49	34.66	αγ	EBEB+BEBE (m)
34.33	34.16	$\alpha\delta^+$	EBEE+EEBE
34.01		$\alpha\delta^+$	BBEE+EEBB
30.92	30.92	γγ	BEEB
30.47	30.48	$\gamma\delta^+$	BEEE+EEEB
29.98	29.98	$\delta^+\delta^+$	$(EEE)_n$
27.70		$2B_2$	BBB (mm)
27.27	27.36	$\beta\delta^+$	EBEE+EEBE
26.8-	27.4-	$2B_2^+$	EBB+BBE (mm)+

(continued)

TABLE 12 (continued)

Chemical shift ppm, TMS		Carbon assignment	Sequence assignment
TCB	TCE-d_2		
27.1	26.8	$\beta\delta^+$	BBEE+EEBB (m)
26.68	26.83	$2B_2$	EBE
24.54	24.71	ββ	EBEBE (m)
24.39		ββ	EBEBB+BBEBE (mm)
24.24		ββ	BBEBB (mmm)
11.18	11.30	Methyl	EBE
11.00	11.12	Methyl	EBB+BBE (m)
10.81		Methyl	BBB (mm)

[a] Assignment tentative.

shift assignments for contiguous 1-butene sequences were confirmed from an essentially isotactic poly-1-butene, which gave the following four resonances:

Carbon type	Sequence	Chemical shift (wrt TMS)
αα Methylene	BBBB (mmm)	40.20 ppm
Methine	BBB (mm)	34.98
$2B_2$ Methylene	BBB (mm)	27.70
Methyl	BBB (mm)	10.81

Remaining assignments were established by noting the relationships between resonance intensities and the 1-butene levels over a range of 2.0 to 14.0 mol% [15]. These assignments are uncomplicated by differences in chirality and inversion, and consequently, there has been a general agreement in the literature [65]. An introduction of the various racemic sequences and inversion would greatly complicate the observed ^{13}C-NMR spectra and lead to the same assignment difficulties encountered in the NMR spectra of ethylene–propylene

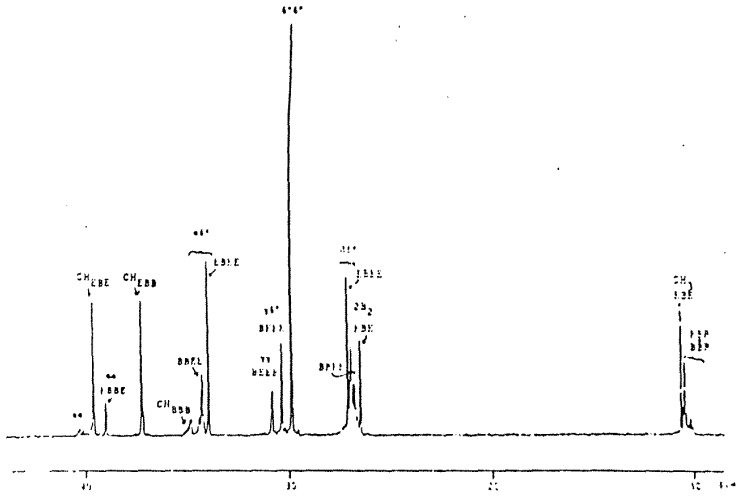


FIG. 9. 50.3 MHz carbon-13 NMR spectrum of a hydrogenated polybutadiene at 125°C in 1,2,4-trichlorobenzene (model ethylene–1-butene copolymer).

copolymers. The assignments for ethylene–1-butene copolymers are, therefore, only partially complete as the effects of chirality and inversion are still to be established.

The quantitative treatment for obtaining a triad sequence distribution, comonomer mole fractions, average sequence lengths, and sequence numbers will follow the same basic procedure just outlined for ethylene–propylene copolymers. The ^{13}C-NMR spectrum for the ethylene–1-butene copolymer is divided into regions as dictated by resolution and certainty in assignments. Resonance broadening in the $\alpha\gamma$, $\alpha\delta^+$, and $\beta\delta^+$ regions from chemical shift differences produced from long-range structural differences essentially precludes the use of relative peak heights or any independent peak area in these

regions. The methine and branch methylene resonances also overlap badly with nearby polymer backbone methylene resonances. Thus a quantitative treatment based on "collective assignments" is needed to avoid errors from overlap and uncertainties produced by unassigned splittings from longer range effects upon an observed n-ad sequence chemical shift. Consequently, only seven regions are available for quantitative use in the spectra of ethylene–1-butene copolymers. Regions A through G are described below in terms of contributing carbon resonances and related n-ads. As was the case for the ethylene–propylene copolymers, the necessary relationships are used to reduce each region intensity to an expression containing contributing triads only.

Region "A"

Range: 37–40 ppm

Contributing carbons: $\alpha\alpha$ Methylene (Methine)$_{EBE}$

Observed n-ads: BBBB, BBBE+EBBB, EBBE EBE

$$T_A = k(BBBB + BBBE+EBBB + EBBE + EBE) \quad (64)$$

$$= k(BB + EBE) \quad (65)$$

$$= k(BBB + (1/2)[BBE+EBB] + EBE) \quad (66)$$

Region "B"

Range: 37.2 ppm

Contributing carbons (Methine)$_{EBB+BBE}$

Observed n-ads: EBB+BBE

$$T_B = k(EBB+BBE) \quad (67)$$

Region "C"

Range: 33.5–35.5 ppm

Contributing carbons: $\alpha\gamma$, $\alpha\delta^+$ (Methine)$_{BBB}$

Observed n-ads. EBEB+BEBE, BBEB+BEBB EBEE+EEBE, BBEE+EEBB BBB

$$T_C = k(EBEB+BEBE + BBEB+BEBB + EBEE+EEBE + BBEE+EEBB + BBB) \quad (68)$$

$$= k(BE+EB + BBB) \quad (69)$$

$$T_C = k(2BEB + BEE+EEB + BBB) \quad (70A)$$

$$= k(2EBE + EBB+BBE + BBB) \quad (70B)$$

$$= k(BEB + (1/2)[BEE+EEB] + EBE + (1/2)[EBB+BBE] + BBB) \quad (71)$$

In Region "C," the "BEB"- and "BEE"-centered tetrads are observed experimentally, thus the use of the B-centered triads in either Eq. (70B) or (71) will force the sequence numbers determined from each half of the triad distribution to be the same. It is preferable to use Eq. (70A) to define the NMR area of Region "C," which allows an independent check of the quality of the measured NMR resonance areas.

Region "D" Range: 29.5–31.5 ppm
Contributing carbons: $\gamma\gamma$, $\gamma\delta^+$, $\delta^+\delta^+$
Observed *n*-ads: BEEB, BEEE+EEEB, $(EEE)_n$

The following special relationship is once again required to define the "D" area in terms of triads:

$$EEE = (1/2)\delta^+\delta^+ + (1/4)\gamma\delta^+ \quad (72)$$

and

$$T_D = \gamma\gamma + \gamma\delta^+ + \delta^+\delta^+ \quad (73)$$

$$= k(2EEE + BEEB + (1/2)[BEEE+EEEB]) \quad (74)$$

$$= k(2EEE + 1/2[BEE+EEB]) \quad (75)$$

Region "E" Range: 26–28 ppm
Contributing carbons: $\beta\delta^+$, $2B_2$
Observed *n*-ads: EBEE+EEBE, BBEE+EEBB EBE, EBB+BBE, BBB

$$T_E = k[(EBEE+EEBE) + (BBEE+EEBB) + EBE + EBB+BBE + BBB] \quad (76)$$

$$T_E = k(BEE+EEB + EBE + EBB+BBE + BBB) \quad (77)$$

Region "F" Range: 24–25 ppm
Contributing carbons: $\beta\beta$
Observed *n*-ads: BBEBB, BBEBE+EBEBB, EBEBE

$$T_F = k(BEB) \quad (78)$$

Region "G" Range: 10.5–11.5 ppm
Contributing carbons: Methyl
Observed *n*-ads: EBE, EBB+BBE, BBB

$$T_G = k(EBE + EBB+BBE + BBB) \quad (79)$$

Again, the correctness of the above equations can be checked by summing from T_A through T_G, which gives $k(2E + 4B)$ after applying the appropriate necessary relationships. As was the case with ethylene–propylene copolymers, some of these regions may have to be combined if a good baseline is not achieved between regions during spectral integration. The final actual method, therefore, will depend on the particular copolymer being examined and its ethylene to 1-butene ratio. As is, seven equations are available to solve for the six triad concentrations. In practice, it is best to omit Region "G" from a quantitative method because of a long methyl spin-lattice relaxation time [11], which requires use of an inordinately long pulse delay as far as the remainder of the spectrum is concerned. A 10-s pulse delay will satisfy all but the methyl group spin-lattice relaxation requirements. For copolymers with very low 1-butene contents, a shorter methyl relaxation time is observed and it becomes more feasible to use Region "G." As stated previously, each copolymer represents a special case, and there are occasions when appropriate long pulse delays should be used and the methyl resonance intensity utilized in the quantitative analysis. Solving equations for Regions "A" through "F" simultaneously gives (note Eq. 70A was used instead of Eq. 70B or 71):

$$k(EEE) = (1/2)T_D - (1/4)T_E + (1/4)T_A + (1/8)T_B \quad (80)$$

$$k(BEE+EEB) = T_E - T_A - (1/2)T_B \quad (81)$$

$$k(BEB) = T_F \quad (82)$$

$$k(EBE) = 2T_F + T_E - T_B - T_C \quad (83)$$

$$k(EBB+BBE) = T_B \quad (84)$$

$$k(BBB) = T_C - 2T_F - T_E + T_A + (1/2)T_B \quad (85)$$

There is a difficulty encountered with the use of the above equations for determining triad distributions for copolymers with 1-butene contents below 5 mol%. Equation (85) for $k(BBB)$ depends upon five different experimental measurements, consequently there is an unacceptable margin of error for the triad with the lowest concentration. In these cases it is better to use T_G and increase the pulse delay appropriately. As stated previously, the spin-lattice relaxation time has decreased somewhat for these methyl resonances when the 1-butene content is fairly low. The use of T_G leads to the following set of equations for the triad distribution:

$$k(EEE) = (1/2)T_D - (1/4)T_E + (1/4)T_G \quad (86)$$

$$k(BEE+EEB) = T_E - T_G \quad (87)$$

$$k(BEB) = T_F \quad (88)$$

$$k(EBE) = T_C - T_A - (1/2)T_B \quad (89)$$

$$k(EBB+BBE) = T_B \quad (90)$$

$$k(BBB) = 2T_A - 2T_C \quad (91)$$

From an experimental standpoint, the above set of equations for the E/B triad distribution leads to a much improved result because the maximum number of experimental observations for any particular triad measurement is three. Fortunately, three observations are required for two of the major triads. Even though the NMR experiment is more time-consuming, a pulse

delay sufficiently long to give reliable methyl intensities will lead to a far more accurate triad distribution.

Normalization of the above equations removes the NMR constant, k, and gives the triad fractions. Number-average sequence lengths, sequence numbers, and run numbers can be obtained from the appropriate equations described earlier for ethylene–propylene copolymers. Because ethylene–1-butene copolymers do not give as many resolvable regions as observed for ethylene–propylene copolymers, there are not as many cross checks available for internal consistency. Considerable care should be given to obtain data that are not biased by baseline contributions from neighboring regions. If it is necessary, a diad distribution can be obtained through the necessary relationships to produce reliable average sequence lengths and comonomer mole fractions. An example of such a necessity will be given later in analyses of ethylene–vinyl acetate copolymers. It should now be clear that one of the advantages of sequence distribution analyses is that each n-ad distribution reduces ultimately to the same information, therefore it is important to obtain the most reliable n-ad distribution and not necessarily the longest n-ad distribution when determining mole fractions, sequence numbers, run numbers, and average sequence lengths.

Polymer chemists are usually more interested in the structural information derived from an n-ad distribution than they are in the n-ad distribution itself. It has already been shown how mole fractions, average sequence lengths, run numbers, and sequence numbers can be determined from any particular n-ad distribution. There is other useful information that can be determined from an n-ad distribution. One of the ethylene–1-olefin structural characteristics of interest is how well a secondary comonomer is dispersed among the primary repeat units in a predominantly ethylene-containing copolymer. Such information is inherently contained within any n-ad distribution. What is needed is a single parameter that would be useful in correlations with physical properties and to differentiate structures produced from combined effects of the catalyst and process employed to make the copolymer. One of the reference points for a particular comonomer distribution is the random or Bernoullian distribution. In the above example, it would be desirable to determine if the 1-butene units are more or less "clustered" than observed for a random distribution. Two approaches have been developed to indicate the degree of "clustering" of 1-olefin units in an ethylene–1-olefin copolymer: one involves a direct empirical measurement of "clustering" and the second utilizes the Bernoullian distribution as a reference

point. The first is the "monomer dispersity," which is simply the ratio of the sequence number to the total 1-olefin content, that is,

$$\text{Monomer dispersity} = (\text{sequence number})/(X) \quad (92)$$

If all of the 1-olefin repeat units are incorporated as EXE, the "monomer dispersity" will be 100. Such is the case for alternating copolymers and medium density ethylene–1-olefin copolymers where the 1-olefin content is less than 3 mol%. Any "clustering" of the 1-olefin units to form contiguous blocks of 1-olefin units leads to monomer dispersities less than 100. It should be noted that Eq. (92) is simply 100 over the average sequence length for "X" and, therefore, does not represent anything new. It is still a useful concept and has the advantage of the greatest accuracy at values closer to 100. The largest errors in monomer dispersity will occur for values between 0 and 1, which occur for average sequence lengths of 100 and higher.

The "cluster index" utilizes the Bernoullian distribution as a reference point for establishing the degree of blocked 1-olefin units in an ethylene–1-olefin copolymer, that is,

$$\text{"Cluster index"} = 10.0\left[1 - \frac{(EXE)_{obs} - (EXE)_{Bern.}}{(X) - (EXE)_{Bern.}}\right] \quad (93)$$

where

$$(EXE)_{Bern.} = (X)(1 - X)^2 \quad (94)$$

and

$$\text{"Cluster index"} = 10.0[(X) - (EXE)_{obs.}]/[2(X)^2 - (X)^3] \quad (95)$$

The "cluster index" is zero whenever the observed (EXE) is the same as (X) and is 10.0 whenever the observed (EXE) is the same as that predicted for a random distribution. The "cluster index" has a useful range of zero to approximately 20. Any values greater than 20 suffer from the same disadvantage as the monomer dispersity when applying the concept to block copolymers with runs of 100 or greater contiguous units.

Regardless of the characterization method utilized or the choice in how the *n*-ad data should be reduced, the most accurate *n*-ad distribution is required. The quantitative procedures developed here utilize well-defined relative areas for obtaining *n*-ad concentrations that give the best possible attainable result. The use of peak heights is to be avoided unless it can be shown that the spectrum contains uniform line widths at one-half the peak heights and there is no error introduced by overlap.

VII. ETHYLENE–1-HEXENE COPOLYMERS

1-Hexene is another important commercial monomer used in the production of linear low- and medium-density polyethylenes. When 1-hexene is copolymerized with ethylene, butyl branches are produced along the polyethylene backbone. It is, once again, of interest to determine not only the total amount of incorporated 1-hexene but establish the manner in which the butyl branches are distributed among the principally ethylene sequences. 1-Hexene forms fewer contiguous repeat units than 1-butene at comparable feed concentrations but does not produce as many isolated branches as found in the corresponding 1-octene copolymer [66]. Ethylene–1-hexene copolymers have served a useful NMR purpose as reference systems for establishing the butyl branch as the most abundant type of branch observed in low-density polyethylenes produced free radically in high-pressure processes [26, 67–70]. The ^{13}C-NMR spectrum at 50.3 MHz of an ethylene–1-hexene copolymer containing 17.3 mol% 1-hexene is reproduced in Fig. 10. Such an ethylene–1-hexene copolymer is of little value commercially but it is a valuable reference system because an opportunity is given to observe nearly all of the possible unique triad and tetrad arrangements possible for ethylene and 1-hexene [71]. A tabulation of chemical shifts and assignments is given in Table 13. Once again this copolymer was prepared with a catalyst system that does not give rise to inverted 1-hexene sequences and produces principally isotactic contiguous 1-hexene sequences.

The majority of assignments in Table 13 could be confirmed through model copolymer systems. One homopolymer of value is poly(1-hexene), which gave the chemical shift assignments

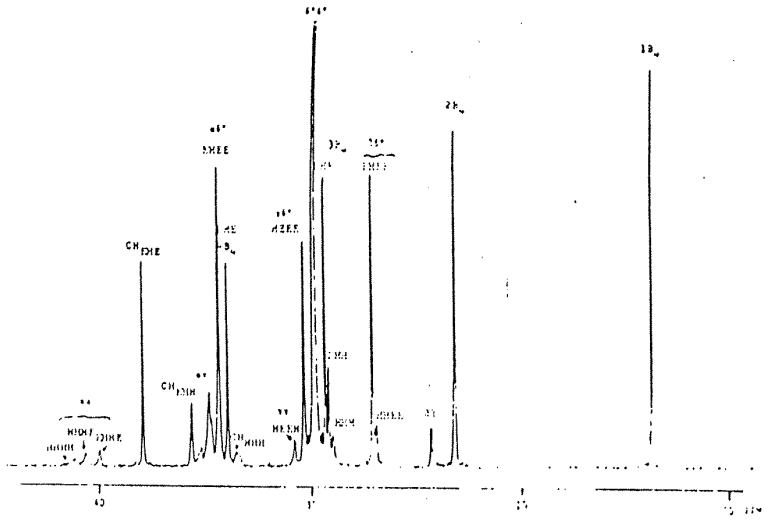


FIG. 10. 50.3 MHz carbon-13 NMR spectrum of an 83/17 ethylene–1-hexene copolymer at 125°C in 1,2,4-trichlorobenzene.

listed in Table 14. It provided confirmation for six chemical shift assignments associated with all contiguous 1-hexene repeat units for the 83/17 copolymer spectrum reproduced in Fig. 10. The ^{13}C-NMR spectrum of poly(1-hexene) has another interesting feature vividly illustrated in Fig. 11. Although spectral integration demonstrated that the six resonances have similar peak intensities, no two resonances in Fig. 10 display the same peak height. The use of peak heights in this homopolymer spectrum would lead to erroneous quantitative measurements.

Similar variations in resonance line widths are also possible for the copolymers, thus the use of peak heights in quantitative determinations is to be strongly discouraged. A second model copolymer containing only 1.9 mol% 1-hexene permitted assignments for all the sequences containing isolated 1-hexene units, that is, EHE, EHEE+EEHE, HEEE+EEEH, etc. Chemical shift data are given for this system in Table 15. Thirteen

TABLE 13

Carbon-13 NMR Chemical Shift Assignments at 50.3 MHz for Ethylene–1-Hexene Copolymers Containing Principally Isotactic 1-Hexene Sequences and No Inverted 1-Hexene Repeat Units. The Samples Were Prepared at 10% by Weight in 1,2,4-Trichlorobenzene (TCB) with Perdeuterobenzene Added and at 15% by Weight in Tetrachloroethane-d_2 (TCE-d_2). The Spectra Were Obtained at 125 ± 1°C. The $\delta^+\delta^+$ Peak Is Set at 29.98 ppm with Respect to an Internal Tetramethylsilane Standard

Chemical shift ppm, TMS		Carbon assignment	Sequence assignment
TCB	TCE-d_2		
41.40			HHHHH (mmm)
40.86			HHHHE+EHHHH (mm)
40.18			EHHHE (m)
38.13	38.22	Methine	EHE
35.85	35.92	Methine	EHH+HHE (m)
35.37		$4B_4$	HHH (mm)
35.00	35.10		HHEH+HEHH (mm)
			EHEH+HEHE (m)
34.90	35.02	$\alpha\delta^+$	HHEE+EEHH
		$4B_4$	EHH+HHE (mm)
34.54	34.62	$\alpha\delta^+$	EHEE+EEHE
34.13	34.21	$4B_4$	EHE
33.57		Methine	HHH (mm)
30.94	30.94		HEEH
30.47	30.48	$\gamma\delta^+$	HEEE+EEEH
29.98	29.98	$\delta^+\delta^+$	$(EEE)_n$

(continued)

Case 1:05-cv-00737-JJF Document 160-6 Filed 09/03/2008 Page 12 of 41

EXHIBIT PAGE 001027

TABLE 13 (continued)

Chemical shift ppm, TMS		Carbon assignment	Sequence assignment
TCB	TCE-d_2		
29.51	29.58	$3B_4$	EHE
29.34	29.41	$3B_4$	EHH+HHE (m)
29.18	29.24	$3B_4$	HHH (mm)
27.28	27.31	$B\delta^+$	EHEE+EEHE
27.09	27.13	$B\delta^+$	HHEE+EEHH (m)
24.53	24.60	BB	EHEHE (m)
24.39		BB	EHEHH+HHEHE (mm)
24.25		BB	HHEHH (mmm)
23.37	23.39	$2B_4$	EHE+EHH+HHE+HHH
14.12	14.21	Methyl	EHE+EHH+HHE+HHH

of the 24 observed resonances reported in Table 13 could be uniquely assigned through observations from these reference homopolymer and copolymer spectra. Five more assignments could be made from trends established in the homologous ethylene–1-olefin copolymer series. In particular, some of the tetrad and pentad sequences have the same chemical shifts independently of the length of the side-chain branch. They are affected only by the position of a branch and not by branch length for those branches two carbons in length and longer.

Experimentally similar $B\delta^+$, $\gamma\gamma$, $\gamma\delta^+$, and BB chemical shifts were obtained for the ethylene–1-butene and ethylene–1-hexene copolymer systems as shown in Table 16. The Grant and Paul "c" parameter would predict that small separations should occur between the various $B\delta^+$ and BB chemical shifts for ethyl- versus butyl-branched copolymer systems. An observed equivalence is not predicted until the side-chain branches reach a length of three carbons. The observation of equivalent $B\delta^+$, $\gamma\gamma$, $\gamma\delta^+$, and BB chemical shifts for both butyl-branched

TABLE 14

Carbon-13 NMR Chemical Shift Assignments at 50.3 MHz for a Principally Isotactic Poly(1-Hexene) Containing No Inverted 1-Hexene Repeat Units. The Sample Was Prepared at 10% by Weight in 1,2,4-Trichlorobenzene and the Spectrum Obtained at 125 ± 1°C with Respect to an Internal Tetramethylsilane Standard

Chemical shift ppm, TMS	Carbon assignment	Sequence assignment
41.38	αα	HHHHH (mmm)
35.29	$4B_4$	HHHH (mm)
33.57	Methine	HHHH (mm)
29.21	$3B_4$	HHHH (mm)
23.52	$2B_4$	HHHH (mm)
14.15	Methyl	HHHH (mm)

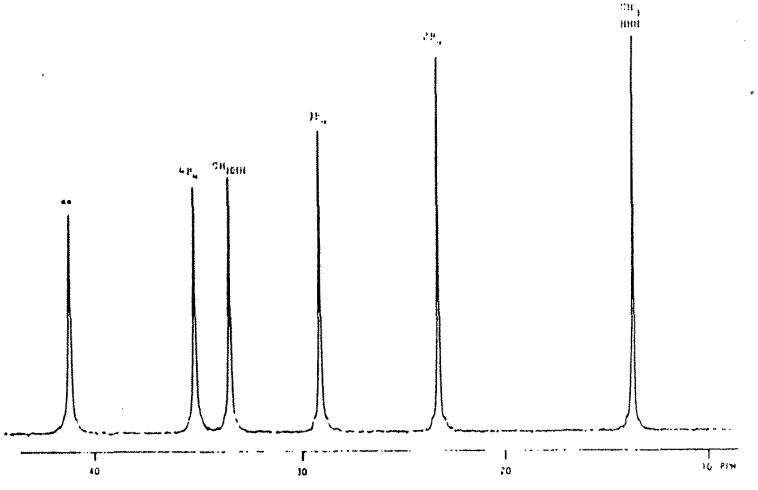


FIG. 11. 50.3 MHz carbon-13 NMR spectrum of an essentially isotactic poly–1-hexene at 125°C in 1,2,4-trichlorobenzene.

TABLE 15

Carbon-13 NMR Chemical Shift Assignments at 50.3 MHz for an Ethylene–1-Hexene Copolymer Containing 1.9 Mol% 1-Hexene. The Sample Was Prepared at 10% by Weight in 1,2,4-Trichlorobenzene and the Spectrum Obtained at 125 ± 1°C with Respect to an Internal Tetramethylsilane Standard

Chemical shift ppm, TMS	Carbon assignment	Sequence assignment
38.14	Methine	EHE
34.53	$\alpha\delta^+$	EHEE+EEHE
34.13	$4B_4$	EHE
30.47	$\gamma\delta^+$	HEEE+EEEH
29.99	$\delta^+\delta^+$	$(EEE)_n$
29.51	$3B_4$	EHE
27.28	$\beta\delta^+$	EHEE+EEHE
23.36	$2B_4$	EHE
14.12	Methyl	EHE

TABLE 16

The $\beta\delta^+$, $\gamma\delta^+$, $\gamma\gamma$, and $\beta\beta$ Sequence Chemical Shifts with Respect to an Internal Tetramethylsilane Standard as Observed in the ^{13}C-NMR Spectra of Ethylene–1-Butene and Ethylene–1-Hexene Copolymers

		Copolymer chemical shifts	
Carbon	Sequence	Ethylene–1-Butene	Ethylene–1-Hexene
$\beta\delta^+$	EXEE+EEXE	27.27	27.28
$\beta\delta^+$	XXEE+EEXX	27.10	27.09
$\gamma\delta^+$	XEEE+EEEX	30.47	30.47
$\gamma\gamma$	XEEX	30.92	30.94
$\beta\beta$	EXEXE	24.54	24.53
$\beta\beta$	EXEXX+XXEXE	24.37	24.39
$\beta\beta$	XXEXX	24.24	24.25

and ethyl-branched copolymers suggests that the Grant and Paul "ε" term derived for alkanes has little, if any, practical use in polymer ^{13}C-NMR chemical shift assignments.

The remaining assignments in Table 13 are made by default. No attempts were made to distinguish among the assignments for the troublesome EHEH+HEHE $\alpha\gamma$ sequences, the EHEE+EEHE $\alpha\delta^+$ sequences, and the $4B_4$ EHH+HHE sequence. These resonances are so close together (within 0.2 ppm) at 50.3 MHz that resolution is virtually impossible. These resonances and assignments are enclosed by parentheses in Table 13. It is significant that it could be established that $\alpha\delta^+$ HHEE+EEHH did occur downfield from the $\alpha\delta^+$ EHEE+EEHE resonance because no obvious methylene resonance occurs above 34.53 ppm. A similar occurrence for the analogous sequence was observed in the ^{13}C-NMR spectra of the ethylene–1-butene copolymers but not for the ethylene–propylene copolymers.

Turning now to a quantitative treatment, we find that the ethylene–1-hexene copolymer spectrum can be conveniently divided into eight spectral regions as indicated by the chemical shift data in Table 13 and the ^{13}C-NMR spectrum in Fig. 9. As was the case for the two previous copolymers, each region is described below in terms of its range in ppm, contributing carbon atoms, and observed n-ad sequences. The final intensity equations for each region are defined by triads only.

Region "A"
Range: 39.5–42 ppm
Contributing carbons: $\alpha\alpha$ Methylene
Observed n-ads: HHHHH, HHHE+EHHHH, EHHE

$$T_A = k(\text{HHHHH} + \text{HHHE+EHHHH} + \text{EHHE}) \quad (96)$$
$$= k(\text{HHH}) \quad (97)$$
$$= k(\text{HHHH} + (1/2)\{\text{HHE+EHH}\}) \quad (98)$$

Region "B"
Range: 38.1 ppm
Contributing carbons: $(\text{Methine})_{\text{EHE}}$
Observed n-ads: EHE

$$T_B = k(\text{EHE}) \quad (99)$$

Region "C"
Range: 33–36 ppm
Contributing carbons: $(\text{Methine})_{\text{EHH+HHE}}$
$(\text{Methine})_{\text{HHH}}$
$4B_4$

Contributing carbons: $\alpha\gamma$

$\alpha\delta^+$

Observed n-ads: EHH+HHE
HHH
EHE+EHH+HHE+HHH
EHEH+HEHE, HHEH+HEHH
EHEE+EEHE, HHEE+EEHH

$$T_C = k(EHEH+HEHE + HHEH+HEHH + EHEE+EEHE + HHEE+EEHH + EHE + 2HHH + 2[EHH+HHE]) \quad (100)$$

$$= k(HE+EH + EHE + 2HHH + 2[EHH+HHE]) \quad (101)$$

$$= k(EHE + 2[EHH+HHE] + 2HHH + 2HEH + [HEE+EEH]) \quad (102)$$

Region "D" Range: 28.5–31 ppm

Contributing carbons: $\gamma\gamma$, $\gamma\delta^+$, $\delta^+\delta^+$
$3B_4$

Observed n-ads: HEEH, HEEE+EEEH, $(EEE)_n$
EHE+EHH+HHE+HHH

$$T_D = \gamma\gamma + \gamma\delta^+ + \delta^+\delta^+ + 3B_4 \quad (103)$$

$$= k(2EEE + (1/2)[HEE+EEH] + EHE + EHH+HHE + HHH) \quad (104)$$

Region "E" Range: 26.5–27.5 ppm

Contributing carbons: $\beta\delta^+$

Observed n-ads: EHEE+EEHE, HHEE+EEHH

$$T_E = k[(EHEE+EEHE) + (HHEE+EEHH)] \quad (105)$$

$$= k(HEE+EEH) \quad (106)$$

Region "F" Range: 24–25 ppm

Contributing carbons: $\beta\beta$

Observed n-ads: HHEHH, HHEHE+EHEHH, EHEHE

$$T_F = k(HEH) \quad (107)$$

Region "G" Range: 23.4 ppm

Contributing carbons: $2B_4$

Observed n-ads: H

$$T_G = k(EHE + EHH+HHE + HHH) \quad (108)$$

Region "H" Range: 14.1 ppm

Contributing carbons: $1B_4$

Observed n-ads: H

$$T_H = k(EHE + EHH+HHE + HHH) \quad (109)$$

Once again, the correctness of the above equations can be established by summing the triad equations for T_A through T_H, which is

$$\Sigma T_x = \text{NMR total area} = 2k(E) + 6k(H) \quad (110)$$

Even though eight equations are available to solve for the six triad fractions, not all of these equations are of the same value experimentally. The equations for T_G and T_H actually measure the (H) monad concentration only. Consideration must also be given to the NMR experimental acquisition conditions because of the length of the side-chain branch, which gives rise to longer relaxation times than encountered in the corresponding ethylene–propylene and ethylene–1-butene copolymers. A 15-s pulse delay was satisfactory for achieving equilibrium conditions for all but the methyl carbons. In this case, meeting the appropriate acquisition conditions for the methyl carbon resonances would not enhance the value of the analysis.

A second factor, which is of consideration in all copolymer *sequence analyses* but not discussed until presently, is the location of endgroup resonances. Generally, ethylene–1-olefin copolymers will have sufficiently high molecular weights for end groups not to make a significant contribution to an overall region intensity. In the case of ethylene–propylene and ethylene–1-butene copolymers, endgroup resonances were sufficiently removed to avoid any complications. Such is not the case for ethylene–1-hexene copolymers where there can be overlap between endgroup and main chain resonances. There

are two major types of end groups in polyethylenes; a straight chain aliphatic end group and a terminal vinyl end group, shown below,

$$-(CH_2)_n-CH_2-CH_2-CH_2-CH_3$$
$$\qquad\qquad\qquad\quad 3s \quad 2s \quad 1s$$

where

1s	14.15 ppm
2s	22.86
3s	32.18

and

$$-CH_2-CH_2-CH_2-CH=CH_2$$
$$\qquad\qquad\quad a \quad 2v \quad 1v$$

where

1v	114.34 ppm (measured in TCE-d_2)
2v	139.46 (measured in TCE-d_2)
a	33.91

The letters "s," "v," and "a" stand for "saturated," "vinyl," and "allylic," respectively. Some catalyst systems give rise to as many as 50% 1-olefin terminal groups while other catalyst systems produce only saturated end groups. The allylic carbon resonance will appear in Region "C" of ethylene–1-hexene copolymers and, in some cases, be obscured by the resonance at 34.13 ppm for the $4B_4$ carbon in EHE sequences. Consequently, an independent technique such as an infrared analysis may be needed to establish the presence of terminal vinyl end groups. When necessary, the overlap problem can be avoided by

eliminating Region "C" from the quantitative treatment as there is still sufficient information to solve for the six triad fractions if the appropriate necessary relationships are utilized. One solution for the triad distribution from the above equations is given below:

$$k(EEE) = (1/2)T_D - (1/2)T_G - (1/4)T_E \quad (111)$$

$$k(EEH+HEE) = T_E \quad (112)$$

$$k(HEH) = T_F \quad (113)$$

$$k(EHE) = T_B \quad (114)$$

$$k(EHH+HHE) = 2T_C - 2T_G - 4T_F - 2T_E - 2T_A \quad (115)$$

$$k(HHH) = 2T_A - T_C + T_G + 2T_F + T_E \quad (116)$$

One of the problems that will be encountered in the use of the above triad equations is that too many independent measurements are required to determine k(EHH+HHE) and k(HHH). For most copolymers where 1-hexene is the minor component, EHH+HHE and HHH will exhibit the lowest concentrations. One improvement can be obtained by factoring the observed Region "C" as follows:

$$T_C = T_{C1} + T_{C2}$$

where

$$T_{C1} = (\text{methine})_{EHH+HHE} = k(EHH+HHE) \quad (117)$$

$$T_{C2} = k(EHE + EHH+HHE + 2HHH + 2HEH + HEE+EEH) \quad (118)$$

The methine resonance for EHH+HHE at 35.83 ppm will often be sufficiently well resolved to be measured independently of the remainder of Region "C." It follows, therefore, that

Case 1:05-cv-00737-JJF Document 160-6 Filed 09/03/2008 Page 16 of 41

EXHIBIT PAGE 001031

$$k(EIIH+HHE) = T_{C1} \quad (119)$$

and

$$k(HIIH) = T_A - (1/2)T_{C1} \quad (120)$$

The Region "T_G" now appears in only one triad equation, and that is for k(EEE). The use of "T_G" in this expression can also be eliminated if deemed necessary. Quite generally, the ethylene–1-hexene copolymers give ^{13}C-NMR data sufficiently overdetermined to provide a number of options when setting up the triad relationships.

Three different ethylene–1-olefin copolymer systems have now been examined for spectral assignments and analytical quantitative procedures. The principles utilized and the approaches required are basically the same. Well-defined spectral regions unaffected by overlap from either endgroup resonances or adjacent "regions" are needed for reliable quantitative results. Normally the system being analyzed will dictate the final approach, and there should be some flexibility on the part of the individual performing an analysis. One last ethylene–1-olefin copolymer, ethylene–1-octene, of importance commercially as a linear low-density polyethylene, will be discussed briefly.

VIII. ETHYLENE–1-OCTENE COPOLYMERS

Copolymerization of 1-octene with ethylene produces a polyethylene with linear hexyl branches distributed along the polymer backbone. The ^{13}C-NMR spectrum of such a copolymer is shown in Fig. 12. Chemical shift assignments are listed in Table 17 for a typical ethylene–1-octene copolymer possessing principally isotactic contiguous 1-octene sequences and no inverted 1-octene repeat units. This spectrum has some strikingly interesting features. First, the three branch carbons, $1B_6$, $2B_6$, and $3B_6$, have chemical shifts that are identical, respectively, to the first three carbon resonances from a linear saturated end group, that is, 1s, 2s, and 3s. The observation

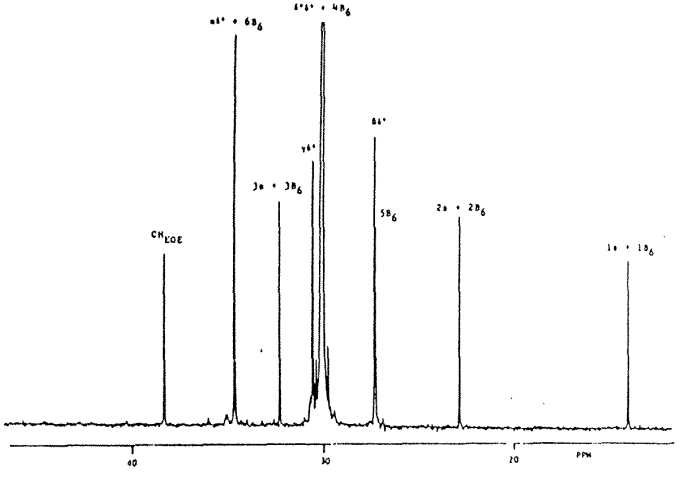


FIG. 12. 50.3 MHz carbon-13 NMR spectrum of an ethylene–1-octene copolymer at 125°C in 1,2,4-trichlorobenzene.

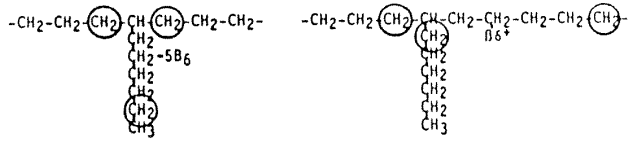
that 3s and $3B_6$ overlap, when predicted to differ by an "ε" effect, again demonstrates that there is no contribution from the Grant and Paul "ε" effect six carbons removed. The remaining branch carbons, $6B_6$, $5B_6$, and $4B_6$, show a close structural correspondence to the $\alpha\delta^+$, $\beta\delta^+$, and $\gamma\delta^+$ carbons, respectively. The resonances from $\alpha\delta^+$ and $6B_6$ overlap perfectly at 34.53 ppm in spectra taken at 50.3 MHz. In contrast, a small separation is observed between the resonances from $5B_6$ and $\beta\delta^+$ as initially reported by Cavagna [72]. This result suggests that an effect from six carbons removed is manifested in this case. The observation that the linear alkane, n-dodecane, produces six distinct ^{13}C-NMR resonances has led to the proposal that chemical shift contributions extend over a

TABLE 17

Carbon-13 NMR Chemical Shift Assignments at 50.3 MHz for a 90/10 Ethylene–1-Octene Copolymer Containing Principally Isotactic 1-Octene Sequences and No Inverted 1-Octene Repeat Units. The Sample Was Prepared at 15% by Weight in Tetrachloroethane-d_2 and the Spectrum Obtained at 125 ± 1°C with Respect to an Internal Tetramethylsilane Standard

Chemical shift ppm, TMS	Carbon assignment	Sequence assignment
40.33	αγ	OOOO (mmm)
38.24	Methine	EOE
35.95	Methine	EOO+OOE (m)
35.09	αγ	OOEO+OEOO (mm)
34.98	αγ	EOEO+OEOE (m)
	αδ+	OOEE+EEOO
34.62	αδ+ + 6B6	EOEE+EEOE
32.22	3s + 3B6	EOE
30.96	γγ	OEEO
30.86		
30.47	γδ+	OEEE+EEEO
29.98	δ+δ+ + 4B6	$(EEE)_n$
27.31	βδ+	EOEE+EEOE
27.27	5B6	EOE
27.09	βδ+	OOEE+EEOO (m)
24.59	ββ	EOEOE (m)
22.89	2s + 2B6	EOE+EOO+OOE+OOO
14.17	1s + 1B6	EOE+EOO+OOE+OOO

range of six carbon atoms [33]. Thus a Grant and Paul "ε" effect was used to calculate alkane chemical shifts. It is interesting that a so-called "six carbon effect" was manifested in the case of the $5B_6$ versus βδ+ carbon resonances but not for the $3B_6$ versus 3s carbon resonances. The difference in this chemical shift behavior likely results from differences in mobility between the polymer backbone and the side-chain alkyl group as pointed out by Tonelli [37, 38]. These two types of side-chain carbons will have "γ" contributions from conformationally dissimilar locations, thus giving rise to a chemical shift difference in the case of the βδ+ and $5B_6$ carbons but not for the $3B_6$ and 3s carbons. The "γ" contribution to $3B_6$ is from a side-chain carbon located at the branch site while the "γ" contribution to 3s is from the sixth carbon from the end of the chain. The difference between these two types of "γ" contributions is not manifested at 50.3 MHz. The three "γ" contributions to $5B_6$ arise from one flexible branch location and two less flexible polymer main-chain locations. The three "γ" contributions to βδ+ arise from two main-chain locations and a less flexible branch location near the main chain as shown below:



γ Carbon Locations for $5B_6$ and βδ+

As a result of these structural differences, it may not be surprising that a chemical shift difference is observed between the $5B_6$ and βδ+ carbon resonances. A similar inspection of the αδ+ and $6B_6$ structural locations shows "γ" contributions from two main-chain locations and one side-chain location in each case. There could be different "γ" contributions from the two

different side-chain locations, but the difference was not sufficient to be manifested at 50.3 MHz. Spectra taken at higher field strengths may show a difference. The chemical shifts for the $\gamma\delta^+$ and the $4B_6$ resonances are not predicted to be close. In fact, $4B_6$ overlaps with the major $\delta\delta^+$ resonance.

There are some expected chemical shift similarities between the ethylene–1-octene copolymers and the ethylene–1-butene and ethylene–1-hexene copolymers, discussed previously. The $\gamma\gamma$, $\gamma\delta^+$, $\beta\delta^+$, and $\beta\beta$ resonances are within experimental error of being the same. It now appears safe to conclude that methylene carbon chemical shifts will be similar for methylene carbons two or more removed from a branch for ethylene–1-olefin copolymers have branches at least two carbons in length. An additional observation, also becoming apparent, is that the various $(\text{methine})_{EXE}$, $(\text{methine})_{EXX+XXE}$, $\alpha\gamma$, and $\alpha\delta^+$ resonances may also be becoming similar for ethylene–1-olefin copolymers with branches four or more carbons in length.

The definition of regions and the development of triad equations for ethylene–1-octene copolymers closely follows that previously developed for ethylene–propylene, ethylene–1-butene, and ethylene–1-hexene copolymers.

Region "A" Range: 39.5–42 ppm
Contributing carbons: $\alpha\alpha$ Methylene
Observed *n*-ads: OOOO, OOOE+EOOO, EOOE

$$T_A = k(OOO + (1/2)[OOE+EOO]) \quad (121)$$

Region "B" Range: 38.1 ppm
Contributing carbons: $(\text{Methine})_{EOE}$
Observed *n*-ads: EOE

$$T_B = k(EOE) \quad (122)$$

Region "C" Range: 36.4 ppm
Contributing carbons: $(\text{Methine})_{EOO+OOE}$
Observed *n*-ads: EOO+OOE

$$T_C = k(EOO+OOE) \quad (123)$$

Region "D" Range: 33–36 ppm
Contributing carbons: $(\text{Methine})_{OOO}$

Contributing carbons: $\alpha\gamma$, $\alpha\delta^+$, $6B_6$
Observed *n*-ads: OOO, EOEO+OEOE, EOEE+EEOE, OOEO+OEOO, OOEE+EEOO, O

$$T_D = k(2(OOO) + [EOO+OOE] + (EOE) + 2(OEO) + [OEE+EEO]) \quad (124)$$

Region "E" Range: 32.2 ppm
Contributing carbons: $3B_6 + 3s$
Observed *n*-ads: O

$$T_E = k(EOE + EOO+OOE + OOO) \quad (125)$$

Region "F" Range: 28.5–31 ppm
Contributing carbons: $\gamma\gamma$, $\gamma\delta^+$, $\delta^+\delta^+$, $4B_6$
Observed *n*-ads: OEEO, OEEE+EEEO, $(EEE)_n$, O

$$T_F = k(2EEE + (1/2)[OEE+EEO] + EOE + EOO+OOE + OOO) \quad (125a)$$

Region "G" Range: 25.5–27.5 ppm
Contributing carbons: $\beta\delta^+$, $5B_6$
Observed *n*-ads: EOEE+EEOE, OOEE+EEOO, O

$$T_G = k(OEE+EEO + EOE + EOO+OOE + OOO) \quad (126)$$

Region "H" Range: 24–25 ppm
Contributing carbons: $\beta\beta$
Observed *n*-ads: OOEOO, OOEOE+EOEOO, EOEOE

$$T_H = k(EOE) \quad (127)$$

Region "I" Range: 22–23 ppm
Contributing carbons: $2B_6 + 2s$

Observed n-ads: O

$$T_I = k(EOE + EOO+OOE + OOO) \quad (128)$$

Region "J" Range: 14–15 ppm
Contributing carbons $1B_6 + 1s$
Observed n-ads: O

$$T_J = k(EOE + EOO+OOE + OOO) \quad (129)$$

Solving the above simultaneous equations for the triad distribution gives:

$$k(EOE) = T_B \quad (130)$$

$$k(EOO+OOE) = T_C \quad (131)$$

$$k(OOO) = T_A - (1/2)T_C \quad (132)$$

$$k(OEO) = T_H \quad (133)$$

$$k(OEE+EEO) = T_G - T_E \quad (134)$$

$$k(EEE) = (1/2)T_F - (1/4)T_E - (1/4)T_G \quad (135)$$

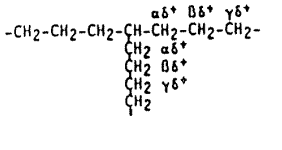
Once again, the system is overdetermined and various combinations can be used depending upon the ^{13}C-NMR acquisition conditions.

Carbon-13 NMR studies of branching in ethylene–1-olefin copolymers at frequencies of 15 and 25 MHz have led to the conclusion that branch lengths six carbons in length cannot be distinguished from those that are longer than six carbons. Frequently, the term "branches, six and longer" describes those linear branches six or more carbons in length. It is clear from the ^{13}C-NMR data generated from an ethylene–1-octene copolymer at 50.3 MHz that branches six carbons in length can now be distinguished from those that are seven and longer. High-frequency measurements may improve this situation even

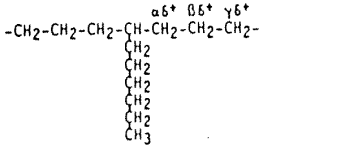
more, but it is not likely that ^{13}C NMR will ever yield a branch length distribution over anything other than the shorter linear branches.

IX. LONG-CHAIN BRANCHING IN POLYETHYLENE

No study on branching and sequence distributions in ethylene–1-olefin copolymers would be complete without a discussion of long-chain branching in polyethylene. The presence of long-chain branching has been clearly evident in low-density polyethylenes prepared by free radical polymerization in high-pressure reactors [68, 73, 74]. An identification of long-chain branches in high-density polyethylenes has been more elusive because of the relatively low amounts that are present [5, 75]. Melt index decreases upon either processing or during conversion of reactor-produced granules to pellets have often been associated with shear-induced long-chain branching. The structure of long-chain branches in polyethylene is called a "Y" type, which gives rise to methine, $\alpha\delta^+$, $\beta\delta^+$, and $\gamma\delta^+$ carbons corresponding to those observed in an ethylene–1-octene copolymer.



"Y" Long Chain Branch in PE



Ethylene-1-Octene Structural Sequence

For this reason, the ethylene–1-octene copolymer serves as a good reference polymer for identifying resonances in high-density polyethylenes associated with long-chain branches. Detection of these resonances in high-density polyethylenes where no 1-olefins were added during polymerization should be strongly indicative of the presence of long-chain branching. Gel permeation chromatography and intrinsic viscosity measurements in connection with ^{13}C-NMR studies can be helpful in deciphering whether or not the "1-octene" types of resonances

detected actually represent long-chain branches [74]. A question that immediately comes to mind is whether or not there is sufficient instrumental sensitivity available to detect long-chain branching in a range of 1 or less per 10,000 carbon atoms in a reasonable time span. A distinct requirement for branching measurements in this range is the availability of sufficient dynamic range during data acquisition. Nuclear magnetic resonance spectrometers, which have 16K computers operating either with double precision arithmetic or utilizing floating point arithmetic during data acquisition, are absolutely required. Otherwise the information leading to branching identification is truncated after only a few data acquisitions. At least a 12–13 bit ADC is necessary and the receiver gain must be properly tuned to ensure the most efficient experiment. Even so, weekend runs with 50 MHz spectrometers are not uncommon.

With a spectral sensitivity sufficient to detect long-chain branching in a range of 1 branch per 10,000 carbon atoms, one finds other benefits that contribute to the polyethylene structural knowledge. Endgroup resonances are usually quite strong as shown in Fig. 13 for a Marlex 6003 polyethylene and unexpected short-chain branches are also identified. Two types of end groups dominate over other types that possibly could be present. They are,

the "saturated" end group $-CH_2-CH_2-CH_2-CH_3$ (3s, 2s, 1s)

the 1-olefin end group $-CH_2-CH_2-CH=CH_2$ (a)

A ratio of the endgroup intensities to the total intensity of the remaining spectral resonances leads to a direct determination of the average carbon number of the polyethylene molecule and, subsequently, to a number-average molecular weight. Carbon-13 NMR is presently the only technique that allows a direct determination of the saturated endgroup concentration with respect to the main chain carbons. The ^{13}C-NMR spectrum of NBS 1475 polyethylene, which has a number-average molecular weight of 18,300 and a weight-average molecular weight of 53,100 is shown in Fig. 14. This NBS standard [76], which is often used in the calibration of gel permeation chromatography columns, is reported to be linear and contain predominantly

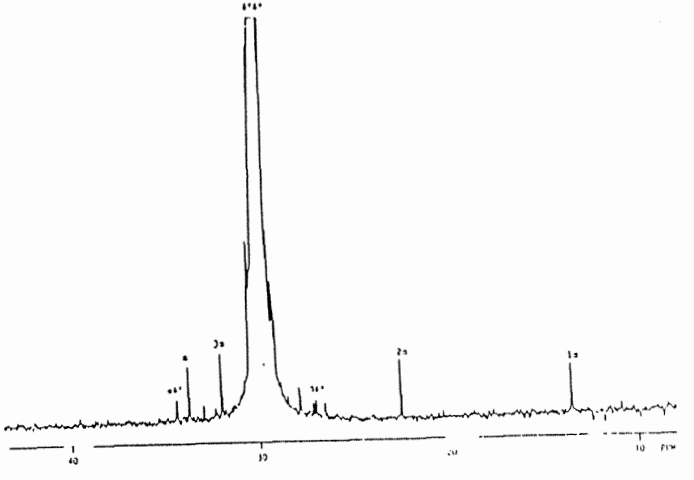


FIG. 13. 50.3 MHz carbon-13 NMR spectrum of Marlex 6003 PE at 125°C in 1,2,4-trichlorobenzene.

aliphatic end groups [77]. NMR intensities for the observed ^{13}C resonances are given in Table 18 as peak heights and peak areas.

The number-average molecular weight, M_n, is given by

$$M_n = \frac{\text{total carbon intensity}}{\text{one carbon intensity}} \times 14 \qquad (136)$$

In terms of peak intensities, the number-average molecular weight is given by

$$M_n = \frac{(1s + 2s + 3s + \delta^+\delta^+ + 3a) \times 14}{(1/2)(s + a)} \qquad (137)$$

where s is the average intensity for 1s, 2s, and 3s and the molecule is assumed to be linear.

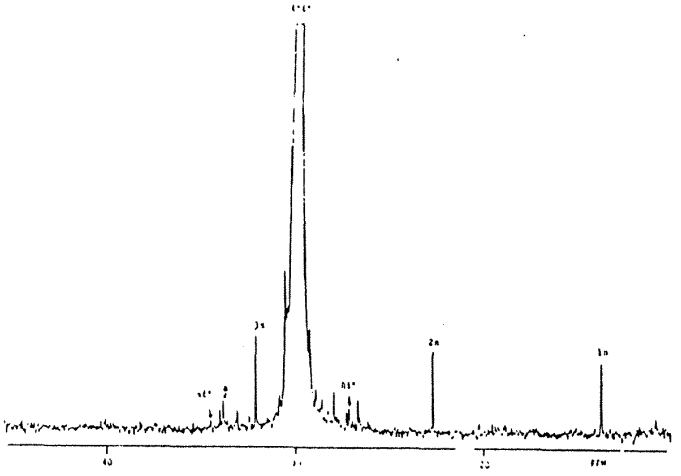


FIG. 14. 50.3 MHz carbon-13 NMR spectrum of NBS 1475 PE at 125°C in 1,2,4-trichlorobenzene.

TABLE 18

Carbon-13 NMR Peak Heights and Integrated Peak Areas for NBS 1475 Polyethylene from a Spectrum Taken in 1,2,4-Trichlorobenzene at 125°C

Carbon	Resonance Intensities	
	By spectral integration	By peak height
1s	0.914	40.5 mm
2s	0.876	50.7
3s	1.043	56.9
$\delta^+\delta^+$	902.402	30,000.0
a	0.484	19.4

Substituting the above peak areas into Eq. (137) gives 17,800 for the number-average molecular weight of NBS 1475. This result is in excellent agreement with the value of 18,300 established by the National Bureau of Standards. The use of peak areas is necessary in this case because the various spectral lines have different line widths at one-half of the peak height. The endgroup resonances typically exhibit line widths at one-half height that are about 20% less than that observed for the major $\delta^+\delta^+$ resonance. It is easy to be deceived by this because, at concentrations of 10% by weight, it is possible to obtain $\delta^+\delta^+$ line widths at one-half height between 1.0 and 1.5 Hz. A line width at one-half height for the NBS 1475 $\delta^+\delta^+$ in Fig. 14 is close to 1.4 Hz. Substituting the NBS 1475 peak height data from Table 18 into Eq. (137) gives a number-average molecular weight of 12,300, which is substantially low. Relative areas by digital integration or a corresponding appropriate method is required when determining polyethylene number-average molecular weights by ^{13}C NMR.

A ^{13}C-NMR spectrum of a polyethylene where long-chain branching could be detected after severe melt processing is shown in Fig. 15. Although butyl branches were originally present, the appearance of resonances associated with long-chain branches is unmistakably evident. The change in composition after processing is given in Table 19. The short-chain butyl branch was unaffected by processing as were the saturated end groups; however, the terminal vinyl group showed a decrease in spectral intensity after processing. From a quantitative viewpoint, sufficient information is available to characterize the degradative process associated with severe processing. The presence of the aliphatic "Y" type of branch suggests that chain scission followed by recombination with nearby secondary radicals is a possible mechanism for long-chain branch formation. The exact nature of this process is still unclear. It is interesting that the loss in terminal vinyl groups corresponds reasonably well to the increase in long-chain branching. A reaction between terminal vinyl groups and secondary free radicals may also offer a plausible explanation for Y-branch formation. The following observations were established:

(a) The number of saturated end groups was not affected by severe melt processing.
(b) The number of terminal vinyl groups was reduced by over 50% after severe melt processing.

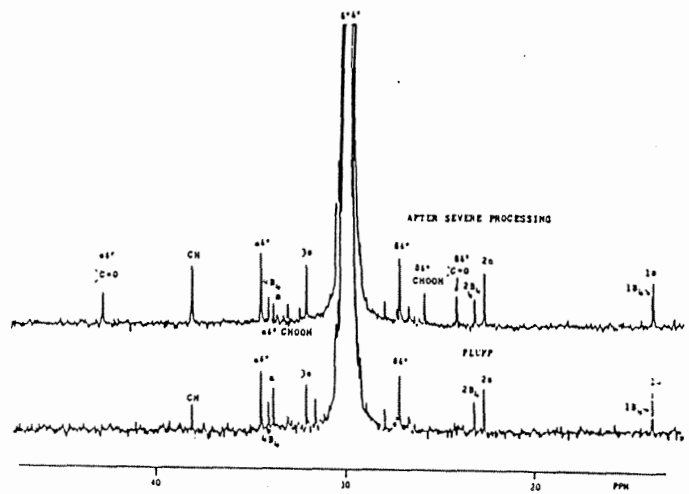


FIG. 15. 50.3 MHz carbon-13 NMR spectrum of a medium-density ethylene–1-hexene copolymer before and after severe processing. The sample was run at 125°C in 1,2,4-trichlorobenzene.

(c) Carbonyl groups and hydroperoxide groups formed after severe melt processing in the presence of air.
(d) Butyl branches were unaffected by severe melt processing.
(e) Long-chain branches formed upon severe melt processing.

The presence of main-chain carbonyl groups was detected by resonances for methylene carbons α and β to the carbonyl group at 42.81 and 24.31 ppm, respectively.

The NMR method for determining number-average molecular weights can be easily adapted to include long-chain branched molecules. The following definitions are needed before setting up the appropriate quantitative relationship:

TABLE 19

Structural Composition of a Medium-Density Ethylene–1-Hexene Copolymer Before and After Severe Melt Processing. The Data Were Determined from Integrated Resonance Intensities from the ^{13}C-NMR Spectrum in Fig. 15. The Sample Was Prepared at 15% by Weight in 1,2,4-Trichlorobenzene and the Spectrum Was Taken at 125°C

	Number of structural units per 10,000 carbons	
Structural unit	Before	After severe processing
Saturated end groups	9.8	10.1
Terminal vinyl end groups	9.6	4.1
Butyl branches	6.8	6.8
Carbonyl groups	Negligible	4.2
Hydroperoxide groups	Negligible	2.4
Long-chain branching[a]	Negligible	3.5

[a]Determined from the $\alpha\delta^+$ resonance intensity after correction for butyl branches.

N = average number of long chain branches per molecule

$N + 2$ = average number of end groups per molecules

s = average intensity for a saturated endgroup carbon

a = the 33.91 ppm allylic carbon atom intensity

α = the average intensity of a carbon from a branch

T_{Tot} = the total carbon intensity

With the above definitions, the polymer carbon number and number-average molecular weight are given as follows:

$$\text{Carbon number} = T_{Tot}(N + 2)/(s + a) \quad (138)$$

$$M_n = 14 \times \text{carbon number} \quad (139)$$

For polymers with long-chain branching and finite values for N, one can take advantage of the following relationship between the intensities of carbons associated with a "Y" type of branch and the endgroup carbons to obtain N:

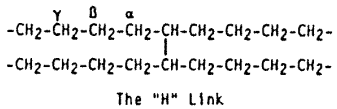
$$N = 2\alpha/[3(s + \alpha) - \alpha] \quad (140)$$

Frequently, long-chain branching is expressed as the number of branches per 1000 or 10,000 carbon atoms as opposed to the number of branches per molecule. In such cases,

$$\text{Branches per 10,000 carbons} = [(1/3)\alpha/(T_{Tot})] \times 10_4 \quad (141)$$

The correct number-average molecular weight by NMR can be used with the weight-average molecular weight by light scattering to characterize the elution behavior of the long-chain branched molecules as observed with gel permeation chromatography. Needless to say, this information is extremely valuable in studies involving correlations with observed physical properties so the time spent in obtaining long-chain branching information is well worth it.

In addition to the "Y" type of long-chain branch, which can be intentionally introduced into a linear polyethylene, it has been considered for some time that the "H" type of branch is introduced into polyethylenes by ionizing radiation [78].



The "H" Link

So far, the only unequivocal ^{13}C-NMR observation of an "H"-link has been after γ-irradiation of n-alkanes [79, 80]. Bennett et al. [79] obtained the following chemical shifts through a study of 1,1,2,2-tetra(tridecyl)ethane and irradiated n-hexadecane and n-eicosane as

α = 30.70 ppm

β = 28.22

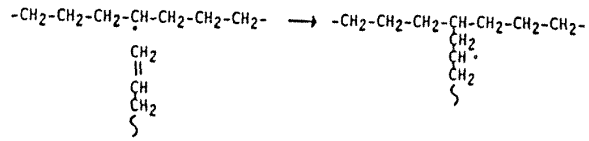
γ = 30.19

Methine = 39.49

Bovey, Schilling, and Cheng [80], in a similar study, identified the "H"-link in a linear alkane ($C_{44}H_{90}$) irradiated in the molten state. No obvious effects could be observed in the ^{13}C-NMR spectrum after irradiation in the crystalline state, although GPC analysis suggested that about 1% of the molecules had doubled in molecular weight. It was concluded that "end-linking" occurred through terminal methyl groups in either adjacent rows or adjacent layers in the crystal structure. In addition to the "H"-link, Bovey and coworkers were able to observe the "Y"-branch after irradiation of the linear alkane in the molten state. It could also be concluded from the NMR data that *trans* double bonds were a product from ionizing radiation. Unfortunately, in an analogous study of polyethylene, Bovey and coworkers were unable to observe either the "H"-link or the "Y"-branch. It was concluded that the introduction of crosslinks at a level sufficient to be detected by NMR led to a system that was too immobile to produce observable, well-defined ^{13}C-NMR resonances.

In a recent irradiation study of a model alkane, Randall, Zoepfl, and Silverman [81] observed the "H"-link and "Y"-branch in an NMR study of n-hexatriacontane irradiated to 100 Mrd in the molten state. In addition, they were able to establish that the methine chemical shift from the "H"-link occurred at 41.0 ppm in 1,2,4-trichlorobenzene at 125°C. Attempts to characterize polyethylenes irradiated past the gel dose were unsuccessful because it became clear that NMR resonances from crosslinked structures were not observable in solution studies of a polyethylene gel. Consequently, a series of irradiations were performed on a Marlex 6003 and NBS 1474 where the amount of radiation employed was intentionally kept below the gel dose [82-84]. It was then that the "Y" branch but not the "H" link could be observed as a product from ionizing radiation. In addition, both *cis* and *trans* double bonds, hydroperoxide groups, and carbonyl groups could be detected. The concentration of saturated end groups appeared to increase with ^{60}Co

γ-irradiation while the terminal vinyl groups showed a marked decrease after irradiation. There was not a material balance between the loss of terminal vinyl groups and the formation of "Y"-branches, thus the mechanism for radiation-induced degradation of polyethylene is still unclear. In a comparison between NBS 1475 and Marlex 6003, it could be concluded that the polyethylene with the higher initial terminal vinyl content produced the greater amount of "Y"-branches with γ-irradiation. Linking between secondary free radicals and terminal vinyl groups is suggested, as shown below:



Carbon-13 NMR spectra of both Marlex 6003 PE and NBS 1475, following a 2.0 Mrd irradiation, are reproduced in Figs. 16 and 17, respectively. The appearance of hydroperoxide groups is indicated by the presence of resonances at 33.14 and 26.83 ppm, respectively, for the α- and β-carbons to the hydroperoxide-substituted methine carbon. If a comparison is made between Figs. 16 and 13, an increase is observed among the resonances associated with long-chain branching that is much greater for Marlex 6003 than for NBS 1475. The increase for NBS 1475 is barely perceptible as indicated by a comparison between Figs. 14 and 17.

Melt irradiations, following thermal degradation in a vacuum at 275°C for an extended time period [83, 84], produce some interesting structural changes in polyethylene. The ^{13}C-NMR spectrum of an irradiated NBS 1475 produced in a two-step process is shown in Fig. 18. The sample was initially heated in a vacuum for 24 h at 275°C prior to a 3.0 Mrd irradiation. The presence of extensive long-chain branchings is clearly evident. In this case the concentration of long-chain branches has reached approximately 44 per 10,000 carbon atoms. Only relatively minor amounts of other components are indicated, that is, *cis* and *trans* double bonds, carbonyl and hydroperoxide groups, and terminal vinyl. A weak 41 ppm resonance is visible and could possibly be assigned to the methine carbons

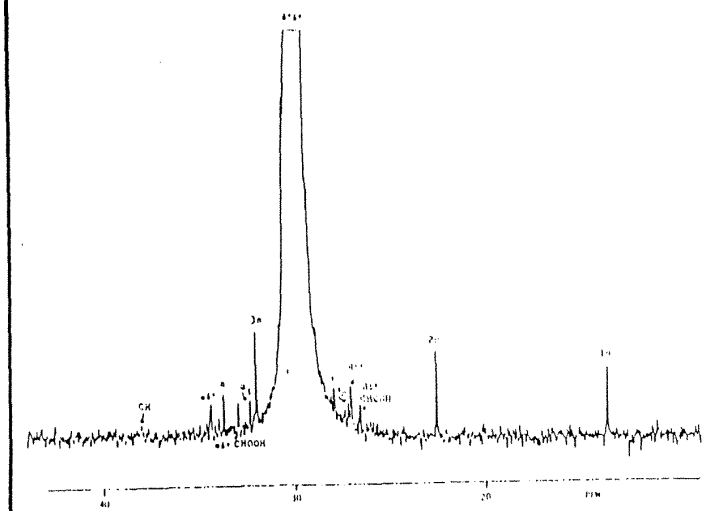


FIG. 16. 50.3 MHz carbon-13 NMR spectrum of Marlex 6003 PE after 2.0 Mrd irradiation at 125°C in 1,2,4-trichlorobenzene.

from a "II"-link. Nevertheless, a preponderance for "Y"-branch formation over "II"-links is indicated under these experimental conditions.

The importance of the disappearance of terminal vinyl groups and its relationship to the gel dose has been previously pointed out by Mandelkern [85]. Lyons [86] has suggested that "Y"-branches could be formed by the reaction between secondary free radicals and terminal vinyl groups, although it has only been in this very recent study that the presence of "Y"-branches following polyethylene irradiations could be demonstrated. The role and importance of the "II"-link is still unclear. It represents a terminating step in a free radical reaction that is ultimately responsible for the formation of rigid, crosslinked structures. The melt-irradiated NBS 1475

Case 1:05-cv-00737-JJF Document 160-6 Filed 09/03/2008 Page 26 of 41

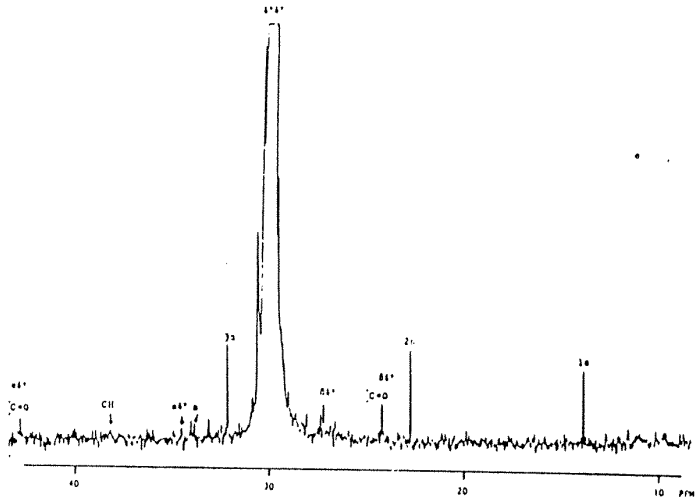


FIG. 17. 50.3 MHz carbon-13 NMR spectrum of NBS 1475 PE after 2.0 Mrd irradiation at 125°C in 1,2,4-trichlorobenzene.

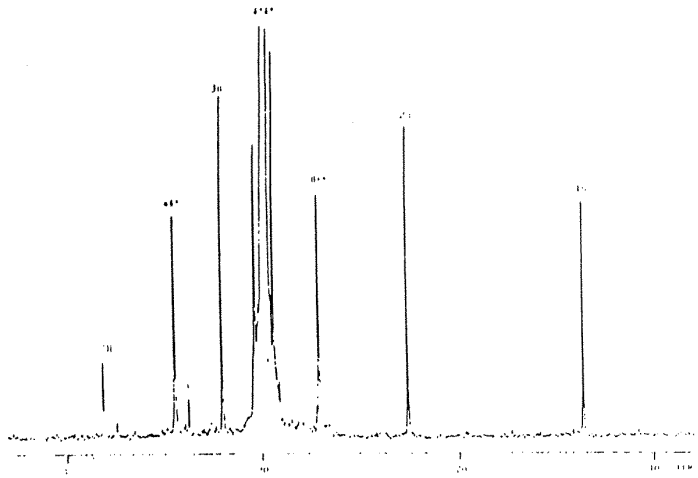


FIG. 18. 50.3 MHz carbon-13 NMR spectrum of NBS 1475 PE after severe thermal degradation in vacuum and subsequent 3.0 Mrd irradiation at 275°C (in 1,2,4-trichlorobenzene at 125°C).

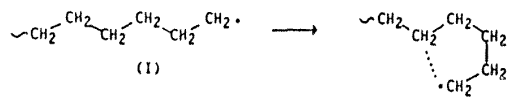
polyethylene in Fig. 18 is free of gel. Some interesting rheological behavior has also been observed for these melt-irradiated systems. A Marlex 6003 PE exhibited a flow activation energy of nearly 41 kcal/mol following thermal degradation in a vacuum at 275°C for 24 h and a subsequent 1.0 Mrd irradiation [87].

X. LOW-DENSITY POLYETHYLENE

Low-density polyethylenes, LDPE, are produced via free radical polymerizations of ethylene in high-pressure tubular and autoclave reactors. The structures are quite complex, containing a variety of short-chain branches in addition to long-chain "Y" types of branches. The principal types of

EXHIBIT PAGE 001041

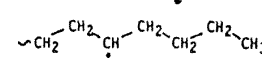
short-chain branches include amyl, butyl, 1,3-diethyl, and 2-ethylhexyl. Even more complicated branching structures involving quaternary carbons have been identified [67]. Roedel [88] proposed what is now a classical backbiting free radical mechanism to account for the existence of amyl, butyl, and long-chain branches in low-density polyethylenes.



(I)

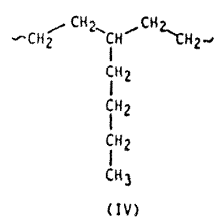
(II)

A Five Membered Transition State



(III)

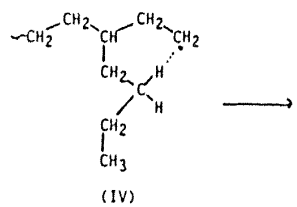
Ethylene



(IV)

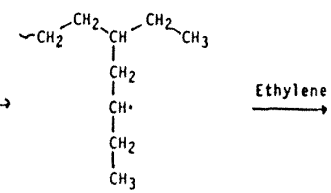
An Isolated Butyl Branch

Amyl branches are produced by a similar mechanism to that presented above, but a six-membered transition state is involved in the backbiting step. Long-chain branches are produced by a corresponding intermolecular chain transfer step. Virtually all of the various short-chain branches observed in low-density polyethylenes can be predicted by successive backbiting steps. Willbourn [89] has extended Roedel's backbiting free radical mechanism to account for 1,3-diethyl branches and 2-ethylhexyl branches.

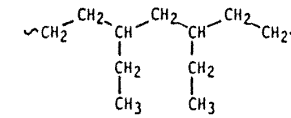


(IV)

A Five Membered Transition State

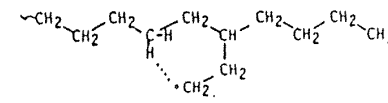


Ethylene



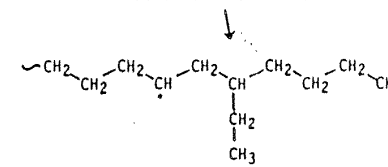
A 1,3-Diethyl Branch

The 2-ethylhexyl branch is formed in a manner analogous to 1,3-diethyl branches, but the backbiting takes place along the main chain instead of the butyl branch:

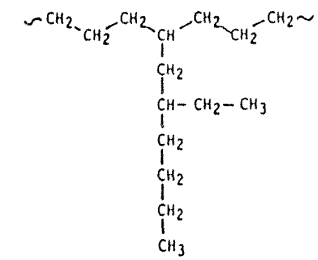


(IV)

A Five Membered Transition State



+ Ethylene



A 2-Ethylhexyl Branch

The advent of ^{13}C NMR removed much of the controversy surrounding the identification of the short-chain branches in low-density polyethylenes with unequivocal identifications of ethyl [26, 67, 68], butyl [26, 67, 68], amyl [26, 68, 90], 1,3-diethyl [68], and 2-ethylhexyl [68] branches. Bowmer and O'Donnell have compared the short-chain branch distribution observed with ^{13}C NMR to the distribution of volatile alkanes obtained after γ-irradiation [91]. By utilizing gel permeation chromatography in conjunction with ^{13}C NMR, Bovey and coworkers [73] were able to confirm the presence of long-chain branches. This result was also supported by Foster who utilized low-angle laser light scattering in addition to GPC and NMR in an independent study [74]. Axelson et al. [68] identified the presence of long-chain branches along with paired ethyl branches and 2-ethylhexyl branches. A ^{13}C-NMR spectrum of a high-pressure, low-density polyethylene is reproduced in Fig. 19. A complete listing of chemical shift assignments is given in Table 20.

Considerable controversy [2, 68] still surrounds the Willbourn mechanism because it implies that ethyl branching should be more abundant than butyl branching, contrary to the majority of the results reported in the literature. Branch distributions, as reported by Bovey [2] and Axelson et al. [68], are tabulated in Table 21.

It is noteworthy that both methyl and propyl branches are typically absent in low-density polyethylenes. Methyl branches are produced only when propylene monomer is added as a chain transfer agent to control both crystallinity and molecular weight [70]. Also, the only time ethyl branches appear as isolated branches is when 1-butene is used as a chain transfer agent. Otherwise, ethyl branches are always present in conjunction with another branch. Mattice and Stehling [92] have accounted for many of the structural features in low-density polyethylenes, which include the absence of methyl and propyl branches as well as the presence of 1,3-diethyl and 2-ethylhexyl branches, using a rotational isomeric state model. These authors concluded that long-chain branching, as estimated exclusively by ^{13}C NMR, is too high and that branches of an intermediate length contribute to the resonance used in ^{13}C-NMR studies of long-chain branching in low-density polyethylenes.

Although studies utilizing ^{13}C NMR to measure branching in low-density polyethylenes have produced an abundance of information about the identity of the various short-chain branches, the air has not yet been cleared of the controversies

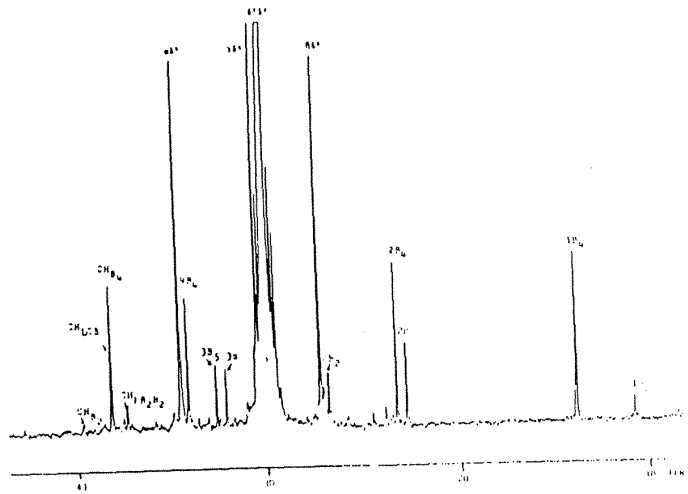


FIG. 19. 50.3 MHz carbon-13 NMR spectrum of NBS 1476 in 1,2,4-trichlorobenzene at 125°C.

surrounding the mechanisms of how these branches are produced [93, 94]. Part of the problem is due to the variabilities in structures of various LDPE's and the lack of information in describing how they are made. Studies relating reaction conditions to structure are now being reported [94].

There were many who believed that the commercial development of linear low-density polyethylenes during the past 15 years would lead to a decline in the production and end use of low-density polyethylenes. The contrary has been true. Copolymers, prepared from ethylene and various vinyl monomers that would act as poisons in Ziegler polymerizations, have led to a resurgence in free radically produced polyethylenes in high-pressure processes. Softness, cling, and clarity in films produced from various copolymers of ethylene and vinyl acetate, vinyl acrylate, methyl methacrylate, and others have opened

TABLE 20

Carbon-13 NMR Chemical Shift Assignments at 50.3 MHz for a Typical Low-Density Polyethylene Produced Free Radically in a High-Pressure Process. Propylene Was Used as a Chain Transfer Agent. The Sample Was Prepared at 15% by Weight in Tetrachloroethane-d_2 and the Spectrum Was Obtained at 125 ± 1°C with Respect to an Internal Tetramethylsilane Standard

Chemical shift ppm, TMS	Carbon assignment	Branch assignment
7–11	$1B_2$	Ethyl
11.12	$1B_2$	1,3-Diethyl
14.02	1s	Amyl+
14.21	$1B_4$	Butyl
20.11	$1B_1$	Methyl[a]
22.89	2s ($2B_{5+}$)	Amyl+
23.39	$2B_4$	Butyl
23.64	$2B_7$(?)	2-Ethylheptyl(?)
24.00	$2B_6$(?)	2-Ethylhexyl(?)
26.92	$2B_2$	1,3-Diethyl
27.31	$\beta\delta^+$	Butyl+
29.98	$\delta^+\delta^+$	$(CH_2)_n$
32.21	3s ($3B_{6+}$)	Hexyl+
32.72	$3B_5$	Amyl
33.29	$(Methine)_{B1}$	Methyl[a]
34.23	$4B_4$	Butyl
34.62	$\alpha\delta^+$	Butyl+
37.41	$(Methine)_{B2}$	1,3-Diethyl
37.58	$\alpha\delta^+$	Methyl[a]
38.22	$(Methine)_{B4}$	Butyl
38.25	$(Methine)_{B4+}$	Butyl+

[a]Propylene used as a chain transfer agent.

TABLE 21

The Branching Distribution in Low-Density Polyethylene as Measured Independently by Bovey [2] and Axelson, Levy, and Mandelkern [68]

Branch type	DNDC polyethylene branches/1000 C [2]	Branch distribution [68]
Ethyl	2.5	12–57%
Butyl	10.9	20–58%
Amyl	3.7	"Lowest"
Hexyl+	4.5	15%
Total	21.6	8–25 Branches/1000 C

the door to many new applications. Four major end-use categories have developed for ethylene–vinyl acetate copolymers: film, adhesives and coatings, molding and profile extrusion, and compounding. The molecular structures of these copolymers can be quite complex. In addition to the sequence distributions typical of copolymers, the free radical backbiting mechanisms still take place, leading to the usual distribution of the various alkyl branches as well as long-chain branching. The following section contains a discussion of ^{13}C-NMR analyses of ethylene–vinyl acetate copolymers where the diad and triad sequence distributions are determined independently of the presence of short-chain branches. In addition, the short-chain branch distribution is also determined for comparison with corresponding low-density polyethylenes.

XI. ETHYLENE–VINYL ACETATE COPOLYMERS

Ethylene–vinyl acetate copolymers form a special problem for ^{13}C-NMR analysis because a combination of events occurs during free radical polymerization in a high-pressure process. First, the vinyl acetate monomers copolymerize with ethylene, forming the various types of sequences anticipated for any copolymer involving ethylene and another monomer. Second, the normal free radical backbiting mechanisms also occur during

copolymerization and lead to the same variety of short-chain branches observed in low-density polyethylenes. A number of workers [95–97] have reported ^{13}C-NMR assignments and quantitative treatments of the sequence distributions occurring in ethylene–vinyl acetate copolymers. Wu et al. determined the ethylene–vinyl acetate comonomer distribution in a series of copolymers to be Bernoullian [95].

One of the problems encountered by early workers in characterizing ethylene–vinyl acetate copolymers was NMR spectrometer sensitivity. The ethylene–vinyl acetate triad distributions were reported without determining the additional ways ethylene was distributed. For example, it would be interesting to report the short-chain alkyl branch distribution along with the ethylene and vinyl acetate contents. Later generations of NMR spectrometers now permit this ethylene distribution to be determined although there is no such report in the open literature. In the following method, the ethylene content listed in the triad distribution will also contain contributions from short-chain branches. The method for acquiring this information will be given in detail. The ethylene distribution over ethyl, butyl, amyl, and hexyl+ branches will also be measured independently of the vinyl acetate content. It is important to have such information because the melting behavior of ethylene–vinyl acetate copolymers depends not just upon the vinyl acetate content but also upon the collective concentration of short-chain branches.

A ^{13}C-NMR spectrum at 50.3 MHz of an ethylene–vinyl acetate copolymer containing approximately 5 mol% vinyl acetate is reproduced in Fig. 20. Chemical shift assignments of key resonances associated with the vinyl acetate comonomer are given in Table 22. The alkyl branch chemical shifts have been discussed previously and are not included in Table 22.

As seen in Fig. 20, the NMR spectral region from 0 to 50 ppm is quite complex, with considerable overlap occurring among the various methylene resonances. The methine and carbonyl resonances are the only ones that are conveniently located for quantitative purposes. The carbonyl region is not so useful as the methine region because longer pulse delays are required if the data are to be acquired under equilibrium conditions. The methine region, which shows at least a nice triad sensitivity, can be used to generate data for the V-centered triads, that is, VVV, VVE+EVV, and EVE,

$$I_{73-74} = kEVE \qquad (142)$$

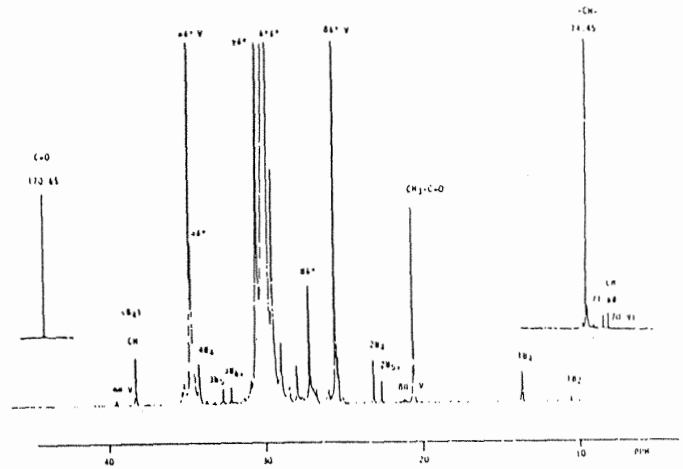


FIG. 20. A carbon-13 NMR spectrum of a 95/5 ethylene–vinyl acetate copolymer at 50.3 MHz and 125°C in tetrachloroethane-d_2.

$$I_{71-73} = k(EVV+VVE) \qquad (143)$$

$$I_{67-69} = kVVV \qquad (144)$$

When compared to the remaining spectral intensity, the total methine area from 67 to 74 ppm leads to the total vinyl acetate mole fraction, that is,

$$I_{\text{total methine}} = kV \qquad (145)$$

$$I_{\text{rest}} = 2kV + 2kE \qquad (146)$$

TABLE 22

Carbon-13 NMR Chemical Shift Assignments at 50.3 MHz for a 95/5 Ethylene–Vinyl Acetate Copolymer Produced Free Radically in a High-Pressure Process; The Sample Was Prepared at 15% by Weight in Tetrachloroethane-d_2 and the Spectrum Was Obtained at 125 ± 1°C with Respect to an Internal Tetramethylsilane Standard

Chemical shift ppm, TMS	Carbon assignment	Sequence assignment
170.65	Carbonyl	EVE
170.45	Carbonyl	EVV+VVE
	Carbonyl	VVV
74.45	Methine	EVE
71.68[a]	Methine	EVV+VVE
70.91[a]	Methine	EVV+VVE
67–69	Methine	VVV
39.54	$\alpha\alpha$	VVVV
39.26	$\alpha\alpha$	EVVE
39.16	$\alpha\alpha$	EVVE
34.67	$\alpha\delta^+$	EVEE+EEVE
30.44	$\gamma\delta^+$	VEEE+EEEV
29.98	$\delta^+\delta^+$	$(EEE)_n$
25.68	$\beta\delta^+$	EVEE+EEVE
21.4–21.6	$\beta\beta$	VEV
20.85	Methyl	V

[a] m,r configurational isomers.

The NMR spectral region defined by I_{rest} ranges from 0 to 50 ppm, which does not include the carbonyl region. The above equations can be solved simultaneously to determine the mole fraction of ethylene and vinyl acetate. The primary advantage in obtaining the ethylene concentration in this manner is that the total ethylene content also includes that in both short- and long-chain branches. Second, the total n-ad area for any n-ad distribution is also obtained,

$$\text{Total } n\text{-ad area} = kV + kE \tag{147}$$

Equation (144) and the methine carbon resonance data for the V-centered triads lead to the following equations for the total diad content:

$$kVV = k[VVV + (1/2)(EVV+VVE)] \tag{148}$$

$$k(EV+VE) = 2kEVE + k(EVV+VVE) \tag{149}$$

$$kEE = kV + kE - kVV - k(EV+VE) \tag{150}$$

The diad distribution defined above will also have ethylene concentrations that include contributions from both long- and short-chain branches. There is a temptation to utilize the methylene resonances associated with the EVEE+EEVE, VEEE+EEEV, and $(EEE)_n$ sequences, but these will not contain contributions from the alkyl branches when defining the ethylene content in the various n-ads.

As stated so many times previously, any reliable n-ad distribution can be used to obtain average sequence lengths, run numbers, or sequence numbers. The above diad distribution is available for this purpose but it is not as useful for establishing a conformity to Bernoullian or Markovian statistical behavior. A triad distribution is better for this latter purpose, and it would be interesting to establish the prerequisites for a reliable triad distribution that includes ethylene in all of its forms. The V-centered triad relationships have been given by Eqs. (142)–(144). The E-centered triads will require measurements of VEE+EEV and VEV. The EEE triad can be obtained through the necessary relationship,

$$kEEE = kEE - (1/2)(VEE+EEV) \tag{151}$$

Because it was determined from kEE, kEEE does contain contributions from short- and long-chain branches. The best available source for k(VEE+EEV) is probably from $\beta\delta^+$ at 25.68 ppm. It does not contain contributions from short-chain branches as this will cause a shift from this particular location. A complete description would include contributions from "VRE+ERV" and "VER+REV," where "R" represents a short-chain branch. The former sequence would produce an $\alpha\delta$ type of resonance while the latter would produce a $\beta\beta$ type of resonance. Omitting these contributions will not create too serious an error at the lower vinyl acetate contributions. These resonances probably could be identified by monitoring resonance intensities in these regions versus an increasing vinyl acetate content. For the time being in the present treatment, these contributions will be neglected. The VEV concentration can be determined from the $\beta\beta$ resonances located at 21.4–21.6 ppm. In this case an omission of the "VRV" types will probably not create any significant error. The magnitude of the errors introduced by these omissions can be established by inspecting the necessary relationships between the diad and triad distributions.

At this point it would be useful to examine the ethylene–vinyl acetate copolymer shown in Fig. 20, quantitatively utilizing the relationships just defined. Carbon-13 NMR intensity data for this copolymer are listed in Table 23.

The monad, diad, and triad distributions calculated from the data in Table 23 are given below. Each measured distribution is reduced progressively to monads through the necessary relationships.

$$[E] = 0.950$$
$$[V] = 0.050$$

$$[EE] = 0.902 \qquad [E] = 0.951$$
$$[EV+VE] = 0.097 \qquad [V] = 0.051$$
$$[VV] = 0.002$$

$$[EEE] = 0.867$$
$$[VEE+EEV] = 0.080$$
$$[VEV] = 0.003$$

$$[EE] = 0.907 \qquad [E] = 0.950$$
$$[EV+VE] = 0.092 \qquad [V] = 0.051$$
$$[VV] = 0.002$$

$$[EVE] = 0.047$$
$$[EVV+VVE] = 0.004$$
$$[VVV] = 0.000$$

TABLE 23

Carbon-13 NMR Integrated Intensities for an 88/12 Ethylene–Vinyl Acetate Copolymer

Resonance	n-ad	Integrated intensity
Methine at 74.5 ppm	EVE	34.1
Methine at 71.6 ppm	EVV+VVE	2.5
Methine at 67.9 ppm	VVV	0.0
Total 0–50 ppm		1463.8
$\beta\delta^+$ Methylene	VEE+EEV	58.0
$\beta\beta$ Methylene	VEV	2.4

The sequence numbers from the diad and triad distributions are

$$1/2(EV+VE) = 0.049$$
$$EVE + 1/2(EVV+VVE) = 0.049$$
$$VEV + 1/2(VEE+EEV) = 0.043$$

Overall, there is good agreement among the diad and triad distributions. The Bernoullian distributions, calculated with the indicated [E], [V] mole fractions, are

$$[EE] = 0.903 \qquad [E] = 0.950$$
$$[EV+VE] = 0.095 \qquad [V] = 0.050$$
$$[VV] = 0.003$$

$$[EEE] = 0.857$$
$$[VEE+EEV] = 0.090$$
$$[VEV] = 0.002 \qquad [E] = 0.950$$
$$[V] = 0.050$$

$$[EVE] = 0.045$$
$$[EVV+VVE] = 0.005$$
$$[VVV] = 0.000$$

As reported by Wu et al. in related systems, good agreement is obtained between the observed and corresponding Bernoullian distributions.

The only remaining concern in determining the above diad and triad distributions is whether an additional correction should be made for inverted vinyl acetate repeat units. Clues could be provided by the presence of an αβ resonance near 29.4 ppm and additional methine resonances near 69 and 73 ppm [98]. Once again, these resonances would require monitoring as a function of increasing vinyl acetate concentration. The [VV] concentration is sufficiently low in the preceding E/V analysis to preclude any significant contribution from inverted vinyl acetate repeat units.

An area that must be considered, as discussed previously in the introduction to this section, is the concentration of the various short-chain alkyl branches. The ethylene content in the preceding methods was carefully defined to include contributions to the total ethylene content from ethylene in short-chain branches when describing the monad, diad, and triad distributions. It is now only necessary to measure the way ethylene units are distributed as ethyl, butyl, amyl, and longer branches. This will be done in terms of branches per 1000 carbon atoms. An expanded ^{13}C-NMR spectrum of the previous 95/5 E/V copolymer is shown in Fig. 20. Resonances are clearly visible for a variety of short-chain branches previously described for low-density polyethylenes and the linear low-density polyethylenes. In particular, resonances for $1B_{4+}$, $1B_2$, $2B_4$, 2s, 3s, and $3B_5$ are distinctly present and offer no greater difficulties in intensity measurements than encountered previously in low-density polyethylenes. The methyl resonances can be used to measure directly the concentrations of ethyl branches and those that are four carbons in length and longer. The concentration of butyl branches only can be measured from the methylene resonance for $2B_4$. Likewise, amyl branches can be measured independently from the intensity of $3B_5$, and hexyl and longer branches can be measured from the intensity of "3s." The methine resonance for B_{4+} at 38.2 ppm can be used as a crosscheck for the total of branches four carbons in length and longer. The chemical shifts for the various alkyl branches observed in ethylene–vinyl acetate copolymers are listed in Table 24.

The degree of overlap and the strength of the major $\delta^+\delta^+$ resonance will dictate the exact route employed when determining

TABLE 24

Observed Chemical Shifts Measured at 50.3 MHz and Assignments for Alkyl Short-Chain Branching in a 95/5 Ethylene–Vinyl Acetate Copolymers Produced in a High-Pressure Process. The Sample Was Prepared at 15% by Weight in Tetrachloroethane-d_2 and the Spectrum Was Obtained at 125 ± 1°C with Respect to an Internal Tetramethylsilane Standard

Chemical shift ppm, TMS	Carbon assignment	Branch assignment
7–11	$1B_2$	Ethyl
14.02	1s	Amyl+
14.07	$1B_4$	Butyl
19.95	$1B_1$	Methyl[a]
22.85	2s ($2B_{5+}$)	Amyl+
23.36	$2B_4$	Butyl
27.30	$\beta\delta^+$	Butyl+
32.16	3s ($3B_{6+}$)	Hexyl+
32.68	$3B_5$	Amyl
33.25	$(\text{Methine})_{B1}$	Methyl[a]
34.17	$4B_4$	Butyl
34.58	$\alpha\delta^+$	Butyl+
37.24	$(\text{Methine})_{B2}$	1,3-Diethyl
37.54	$\alpha\delta^+$	Methyl[a]
38.19	$(\text{Methine})_{B4+}$	Butyl+
39.61	$(\text{Methine})_{B2}$	Ethyl

[a]Propylene used as a chain transfer agent.

the alkyl branch distribution. In general, the total ethyl branching is determined from the $1B_2$ resonance area. The butyl, amyl, and hexyl+ branching is determined from $2B_4$, $3B_5$, and 3s ($3B_{6+}$), respectively. A number of other resonances are available for crosschecks. One good relationship to monitor is

$$2s = 3B_5 + 3s \qquad (152)$$

which permits the influence of overlap from $\delta^+\delta^+$ to be examined. The following results were obtained for the alkyl branching in the 88/12 EVA copolymer:

Branch type	Number per 1000 carbons
Methyl	0.2
Ethyl	1.3
Butyl	3.1
Amyl	1.1
Hexyl+	1.2

The methyl branches occur when propylene is used as a chain transfer agent and are not part of the Roedel process that produces the other types of alkyl branches.

XII. CONCLUSION

The determinations of structure of the various ethylene-containing copolymers discussed throughout this article hopefully illustrate the enormous progress made in polymer characterization through high-resolution liquid ^{13}C-NMR techniques. There are a number of examples of how this structural information can be usefully applied. Sequence distribution measurements permit the relationships between a catalyst recipe and incipient polymer structure to be precisely determined. Structure–property relationships, which will be useful in the future design of polymers for specific applications, can also be established. Precise relationships among melting behavior, crystallinity, and structure of polymers can also now be determined. Correlations between polymer molecular structure and incipient solid-state structure can do a lot to clarify those observed relationships between molecular structure and physical properties. This NMR information, when combined with data from rheology, microscopy, and solid-state structure, can lead to new generations of intelligently designed polymers that will meet specific consumer needs during the next decades.

ACKNOWLEDGMENT

The author expresses his appreciation to Phillips Petroleum Company for its consent to publish this article. The present manuscript is a completely rewritten and updated version of an original article that was written approximately five years ago. At that time, it was released by Phillips Petroleum Company for publication in a monograph dealing with polymer characterization. After the project failed, the original manuscript was returned by the editor and subsequently modified to its present form. Phillips Petroleum Company graciously allowed the original manuscript to serve as a framework for a revised, up-to-date review article.

REFERENCES

[1] J. C. Randall, *Polymer Sequence Determination: Carbon 13 NMR Method*, Academic, New York, 1977.
[2] F. A. Bovey, *Proceedings of China-U.S. Bilateral Symposium on Polymer Chemistry and Physics*, Van Nostrand Reinhold, New York, 1981.
[3] F. A. Bovey, *Polymer Conformation and Configuration*, Academic, New York, 1969.
[4] H. J. Harwood and W. M. Ritchey, *J. Polym. Sci., Part B*, 2, 601 (1964).
[5] J. C. Randall, in *Polymer Characterization by ESR and NMR* (ACS Symposium Series, No. 142) (A. E. Woodward and F. A. Bovey, eds.), American Chemical Society, Washington, D.C., 1980.
[6] A. Zambelli, P. Locatelli, G. Bajo, and F. A. Bovey, *Macromolecules*, 8, 687 (1975).
[7] A. Zambelli, G. Gatti, C. Sacchi, W. O. Crain Jr., and J. D. Roberts, *Ibid.*, 4, 475 (1971).

[8] T. C. Farrar and E. D. Becker, *Pulse and Fourier Transform NMR*, Academic, New York, 1969.
[9] J. Schaefer and D. F. S. Natusch, *Macromolecules*, *5*, 416 (1972).
[10] F. A. Bovey, *High Resolution NMR of Macromolecules*, Academic, New York, 1972, Chap. 1.
[11] D. E. Axelson, L. Mandelkern, and G. C. Levy, *Macromolecules*, *10*, 557 (1977).
[12] J. C. Randall, *J. Polym. Sci., Polym. Phys. Ed.*, *14*, 1693 (1976).
[13] Y. Inoue, A. Nishioka, and R. Chujo, *Makromol. Chem.*, *168*, 163 (1973).
[14] A. Allerhand and R. K. Hallstone, *J. Chem. Phys.*, *56*, 3718 (1972).
[15] E. T. Hsieh and J. C. Randall, *Macromolecules*, *15*, 353 (1982).
[16] K. F. Kuhlmann, D. M. Grant, and R. K. Harris, *J. Chem. Phys.*, *52*, 3429 (1970).
[17] J. J. Dechter, R. A. Komoroski, D. E. Axelson, and L. Mandelkern, *J. Polym. Sci., Polym. Phys. Ed.*, *19*, 631 (1981).
[18] D. Doddrell and A. Allerhand, *J. Am. Chem. Soc.*, *93*, 1558 (1971).
[19] A. Allerhand, D. Doddrell, and R. Komoroski, *J. Chem. Phys.*, *55*, 189 (1971).
[20] *Varian Instruments at Work*, *9-1* (1979).
[21] George Gray, Varian Associates, Private Communication.
[22] C. J. Carman and C. E. Wilkes, *Rubber Chem. Technol.*, *44*, 781 (1971).
[23] C. E. Wilkes, C. J. Carman, and R. A. Harrington, *J. Polym. Sci., Polym. Symp.*, *43*, 237 (1973).
[24] C. J. Carman, R. A. Harrington, and C. E. Wilkes, *Macromolecules*, *10*, 536 (1977).
[25] J. C. Randall, *Ibid.*, *11*, 33 (1978).
[26] J. C. Randall, *J. Polym. Sci., Polym. Phys. Ed.*, *11*, 275 (1973).
[27] S. L. Patt and J. N. Shoolery, *J. Magn. Reson.*, *46*, 535 (1982).
[28] G. A. Morris and R. Freeman, *J. Am. Chem. Soc.*, *101*, 760 (1979).
[29] K. Hikichi, T. Hiraoki, S. Takemura, M. Ohuchi, and A. Nishioka, in *NMR and Macromolecules* (ACS Symposium Series, No. 247) (J. C. Randall, ed.), American Chemical Society, Washington, D.C., 1984, Chap. 8.
[30] G. A. Morris, *J. Am. Chem. Soc.*, *102*, 428 (1980).
[31] D. M. Doddrell, D. T. Pegg, and M. R. Bendall, *J. Magn. Reson.*, *48*, 323 (1982).

[32] P. F. Barron, D. J. T. Hill, J. H. O'Donnell, and P. W. O'Sullivan, *Macromolecules*, *17*, 1967 (1984).
[33] D. M. Grant and E. G. Paul, *J. Am. Chem. Soc.*, *86*, 2984 (1964).
[34] J. C. Randall, *J. Polym. Sci., Polym. Phys. Ed.*, *13*, 901 (1975).
[35] C. J. Carman, A. J. Tarpley Jr., and J. H. Goldstein, *Macromolecules*, *6*, 719 (1973).
[36] L. P. Lindeman and J. Q. Adams, *Anal. Chem.*, *43*, 1245 (1971).
[37] A. E. Tonelli, *Macromolecules*, *12*, 255 (1979).
[38] A. E. Tonelli, *Ibid.*, *11*, 634 (1978).
[39] U. W. Suter and P. J. Flory, *Ibid.*, *8*, 765 (1975).
[40] A. E. Tonelli, *Ibid.*, *11*, 565 (1978).
[41] A. E. Tonelli, *Ibid.*, *12*, 83 (1979).
[42] A. E. Tonelli and F. C. Schilling, *Ibid.*, *13*, 270 (1980).
[43] A. Zambelli, P. Locatelli, G. Bajo, and F. A. Bovey, *Ibid.*, *8*, 687 (1975).
[44] A. Provasoli and D. R. Ferro, *Ibid.*, *10*, 874 (1977).
[45] A. Zambelli, P. Locatelli, A. Provasoli, and D. R. Ferro, *Ibid.*, *13*, 267 (1980).
[46] H. Sato and Y. Tanaka, *ACS ORPL Prepr.*, *48*, 196 (1983).
[47] H. Sato and Y. Tanaka, in NMR and Macromolecules (ACS Symposium Series, No. 247) (J. C. Randall, ed.), American Chemical Society, Washington, D.C., 1984, Chap. 12.
[48] H. J. Harwood, T. Chen, and F. Lin, *Ibid.*, Chap. 13.
[49] M. Moller and H. J. Cantow, *Macromolecules*, *17*, 733 (1984).
[50] M. D. Bruch, F. A. Bovey, and R. E. Cais, *Ibid.*, *18*, 1253 (1985).
[51] M. D. Bruch and J. K. Bonesteel, *Ibid.*, *19*, 1622 (1986).
[52] M. D. Bruch and W. G. Payne, *Ibid.*, *19*, 2712 (1986).
[53] P. A. Mirau, F. A. Bovey, A. E. Tonelli, and S. A. Heffner, *Ibid.*, *20*, 1701 (1987).
[54] S. A. Heffner, F. A. Bovey, L. A. Verge, P. A. Mirau, and A. E. Tonelli, *Ibid.*, *19*, 1628 (1986).
[55] G. J. Ray, P. E. Johnson, and J. R. Knox, *Ibid.*, *10*, 773 (1977).
[56] W. V. Smith, *J. Polym. Sci., Polym. Phys. Ed.*, *18*, 1573 (1980).
[57] W. V. Smith, *Ibid.*, *18*, 1587 (1980).
[58] J. C. Randall and E. T. Hsieh, *Macromolecules*, *15*, 1584 (1982).
[59] H. N. Cheng, *Ibid.*, *17*, 1950 (1984).

[60] L. Zetta, G. Gatti, and G. Audisio, *Ibid.*, *11*, 763 (1978).
[61] J. C. Randall, *Polymer Sequence Determination: Carbon 13 NMR Method*, Academic, New York, 1977, Chap. 4.
[62] J. N. Short, in *Kirk-Othmer Encyclopedia of Chemical Technology*, Vol. 16, Wiley, New York, 1981, p. 385.
[63] A. D. H. Clague, J. A. M. van Broekhoven, and L. P. Blouaw, *Macromolecules*, *7*, 348 (1974).
[64] J. C. Randall, *J. Polym. Sci., Polym. Phys. Ed.*, *13*, 1975 (1975).
[65] G. J. Ray, J. Spanswick, J. R. Knox, and C. Serres, *Macromolecules*, *14*, 1323 (1981).
[66] J. C. Randall and E. T. Hsieh, in *NMR and Macromolecules* (ACS Symposium Series, No. 247) (J. C. Randall, ed.), American Chemical Society, Washington, D.C., 1984, Chap. 9.
[67] D. E. Dorman, E. P. Otocka, and F. A. Bovey, *Macromolecules*, *5*, 507 (1972).
[68] D. E. Axelson, G. C. Levy, and L. Mandelkern, *Ibid.*, *12*, 41 (1979).
[69] M. E. A. Cudby and A. Bunn, *Polymer*, *17*, 345 (1976).
[70] Y. Sugimura, T. Usami, T. Nagaya, and S. Tsuge, *Macromolecules*, *14*, 1787 (1981).
[71] E. T. Hsieh and J. C. Randall, *Ibid.*, *15*, 1402 (1982).
[72] F. Cavagna, *Ibid.*, *14*, 215 (1981).
[73] F. A. Bovey, F. C. Schilling, F. L. McCrackin, and H. L. Wagner, *Ibid.*, *9*, 76 (1976).
[74] G. N. Foster, *Polym. Prepr.*, *20*, 463 (1979).
[75] G. Kraus and C. J. Stucy, *J. Polym. Sci., Polym. Symp.*, *43*, 329 (1973).
[76] *Journal of Research of the National Bureau of Standards*, *76A*(2) (1972).
[77] Leslie Smith, National Bureau of Standards, Private Communication.
[78] G. Ungar, *J. Mater. Sci.*, *16*, 2635 (1981).
[79] R. L. Bennett, A. Keller ,and J. Steiny, *J. Polym. Sci., Polym. Phys. Ed.*, *14*, 3027 (1976).
[80] F. A. Bovey, F. C. Schilling, and H. N. Cheng, in *Advances in Chemistry Series*, No. 169 (D. L. Allara and W. L. Hawkins, eds.), American Chemical Society, Washington, D.C., 1978, Chap. 11.
[81] J. C. Randall, F. J. Zoepfl, and J. Silverman, *Rapid Commun.*, *4*, 149 (1983).
[82] J. C. Randall, F. J. Zoepfl, and J. Silverman, *Radiat. Phys. Chem.*, *22*, 183 (1983).
[83] J. C. Randall, F. J. Zoepfl, and J. Silverman, *ACS ORPL Prepr.*, *48*, 211 (1983).

[84] J. C. Randall, F. J. Zoepfl, and J. Silverman, in *NMR and Macromolecules* (ACS Symposium Series, No. 247) (J. C. Randall, ed.), American Chemical Society, Washington, D.C., 1984, Chap. 16.
[85] L. Mandelkern, in *The Radiation Chemistry of Macromolecules*, Vol. 1 (M. Dole, ed.), Academic, New York, 1972, Chap. 13.
[86] B. J. Lyons, *International Conference on Radiation Processing for Plastics and Rubber*, The Plastics Institute, London, 1981, Chap. 5.
[87] W. M. White, J. C. Randall, and C. H. Leigh, *Chem. Eng. Commun.*, *24*, 139 (1983).
[88] M. J. Roedel, *J. Am. Chem. Soc.*, *75*, 6110 (1952).
[89] A. H. Willbourn, *J. Polym. Sci.*, *34*, 569 (1959).
[90] J. C. Randall, *J. Appl. Polym. Sci.*, *22*, 585 (1978).
[91] T. N. Bowmer and J. H. O'Donnell, *Polymer* (1977).
[92] W. L. Mattice and F. C. Stehling, *Macromolecules*, *14*, 1479 (1981).
[93] D. Stoiljkovich and S. Jovanovich, *Makromol. Chem.*, *182*, 2811 (1981).
[94] D. Stoiljkovich and S. Jovanovich, *J. Polym. Sci., Polym. Chem. Ed.*, *19*, 741 (1981).
[95] T. K. Wu, D. W. Ovenall, and G. S. Reddy, *J. Polym. Sci., Polym. Phys. Ed.*, *12*, 901 (1974).
[96] B. Ibrahim, A. R. Katritzky, A. Smith, and D. E. Weiss, *J. Chem. Soc., Perkins Trans. II*, 1537 (1974).
[97] M. Delfini, A. Segre, and F. Conti, *Macromolecules*, *6*, 456 (1973).
[98] J. C. Randall, *Polymer Sequence Determination: Carbon 13 NMR Method*, Academic, New York, 1977, p. 142.

36

6

Characterization of Long-Chain Branching in Polyethylenes Using High-Field Carbon-13 NMR

J. C. RANDALL

Phillips Petroleum Company, Bartlesville, OK 74004

The simplest polymer molecule examined for both its dynamic and structural characteristics utilizing carbon-13 nuclear magnetic resonance has been polyethylene. At first sight, a polymer molecule which is essentially a "polymethylene" would not seem to possess enough different structural characteristics to warrant more than a casual investigation. However, there are a variety of different polyethylenes available commercially that have substantially different physical properties and, subsequently, different end use applications. The fact that catalysts are sought to produce polyethylenes with desirable properties and that post treatments may be used to alter certain physical characteristics imply that there is a direct link between physical properties and molecular structure. This link between structure and properties and the commercial importance of polyethylene have brought about a need for a thorough structural characterization.

Polyethylenes produced commercially via high pressure, free radical processes have densities around 0.92 g/cc and are referred to simply as "low density" polyethylenes. It has been well established from infrared measurements that these low density polyethylenes possess appreciable quantities of ethyl and butyl branches (1-3) but it was not until C-13 NMR became available that an absolute identification, both qualitatively and quantitatively, of the short branches became possible (4-8). Long chain branching is also present in high pressure process low density polyethylenes and carbon-13 NMR was useful here also in establishing the identity and relative amounts of long versus short chain branches (9-11).

Polyethylenes with densities around 0.96 g/cc are categorized as high density polyethylenes and are prepared using either titanium or chromium based catalysts. These polyethylenes are usually linear although the physical and rheological properties of some high density polyethylenes have suggested the presence of long chain branching (12) at a level one to two orders of magnitude below that found for low density polyethylenes prepared by a high pressure process. A measurement of long chain branching in

0-8412-0594-9/80/47-142-093$06.50/0
© 1980 American Chemical Society

high density polyethylenes has been elusive because of the concentrations involved (13) and can only be directly provided by recently available, high field, high sensitivity NMR spectrometers. The purpose of this chapter will be to review briefly the history of structural studies of polyethylene and show where these recent advances in C-13 NMR instrumentation have greatly enhanced our knowledge about polyethylene structure.

Among the most important polyethylene structural characteristics are the weight and number average molecular weights, M_w and M_n, and the molecular weight distribution characterized by M_w/M_n. Since C-13 NMR can also be used to measure a number average molecular weight, it may be advantageous to examine some of the molecular weight characteristics of polyethylenes. As shown by the size exclusion (or gel permeation) chromatographs in Figure 1, the molecular weight distributions are generally broad but can be significantly characteristic to distinguish among certain types of polyethylenes. For example, the first polymer in Figure 1 has a relatively narrow molecular weight distribution with an M_w/M_n of approximately three. The second polyethylene has a much broader molecular weight distribution with an M_w/M_n of approximately twenty. Finally, the third polyethylene has a distinctly bimodal molecular weight distribution. These size exclusion chromatograms do serve as distinguishing fingerprints for the molecular weight distributions which can only be measured quantitatively by the ratio, M_w/M_n. Recent improvements in size exclusion chromatography techniques have permitted faster and more reliable molecular weight determinations (14).

Polyethylenes prepared with a Ziegler type, titanium based catalyst have predominantly n-alkyl or saturated end groups. Those prepared with chromium based catalysts have a propensity toward more olefinic end groups. As will be seen later, the ratio of olefinic to saturated end groups for polyethylenes prepared with chromium based catalysts is approximately unity. The end group distribution is, therefore, another structural feature of interest in polyethylenes because it can be related to the catalyst employed and possibly the extent of long chain branching. Infrared has been a useful technique for measuring the various types of olefinic end groups (15), which may be

$-CH_2-CH=CH_2$ "vinyl"

$-CH_2-\underset{\displaystyle CH_3}{\overset{\displaystyle |}{C}}=CH_2$ "vinylidene"

$-CH_2-CH=CH-CH_3$ "internal cis or trans"

Figure

the con-
ovided by
pectrome-
iefly the
ow where
greatly

haracter-
ghts, M_w
rized by
a number
nine some
nes. As
graphs in
ly broad
ong cer-
lymer in
ribution
lyethyl-
with an
lyethyl-
ibution.
guishing
ich can
Recent
es have
termina-

m based
groups.
pensity
er, the
es pre-
y. The
feature
to the
branch-
he var-

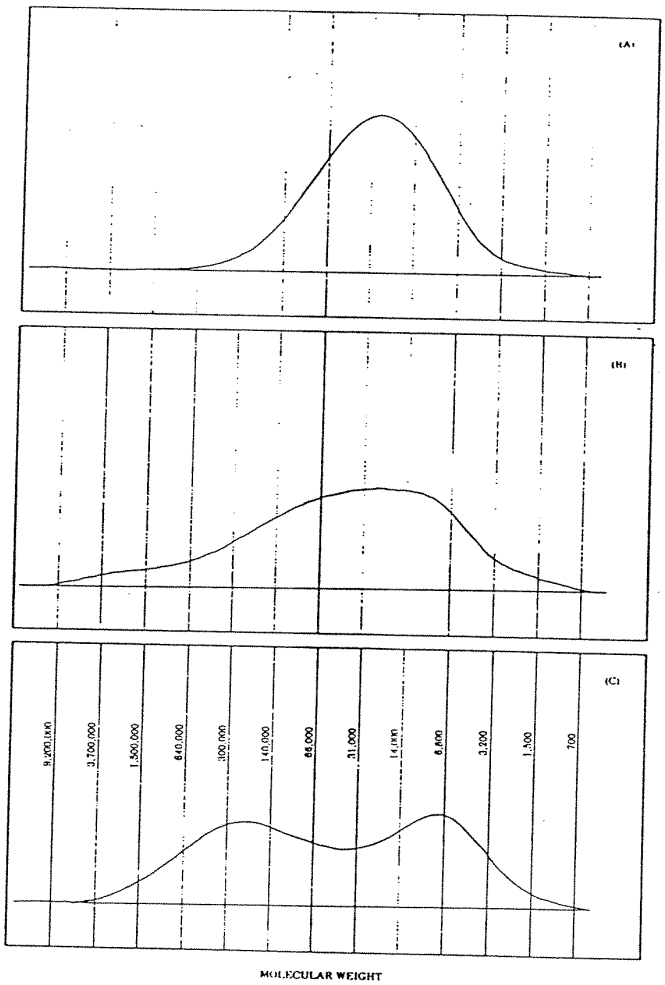


Figure 1. SECs of (A) NBS 1475, (B) Phillips PE 5003, and (C) Hizex 7000

Prior to the availability of C-13 NMR, there was no technique for measuring directly the saturated end group concentration. Now it is possible not only to measure concentrations of saturated end groups, but also the olefinic end groups and, subsequently, an end group distribution.

Short chain branches can be introduced deliberately in a controlled manner into polyethylenes by copolymerizing ethylene with a 1-olefin. The introduction of 1-olefins allows the density to be controlled and butene-1 and hexene-1 are commonly used for this purpose. Once again, as in the case of high pressure process low density polyethylenes, C-13 NMR can be used to measure ethyl and butyl branch concentrations independently of the saturated end groups. This result gives C-13 NMR a distinct advantage over corresponding infrared measurements because the latter technique can only detect methyl groups irrespective of whether the methyl group belongs to a butyl branch or a chain end (16). As will be seen shortly, C-13 NMR also has a disadvantage in branching measurements because only branches five carbons in length and shorter can be discriminated independently of longer chain branches (5)(9). Branches six carbons in length and longer give rise to the same C-13 NMR spectral pattern independently of the chain length. This lack of discrimination among the longer side-chain branches is not a deterring factor, however, in the usefulness of C-13 NMR in a determination of long chain branching.

By far the most difficult structural measurement and, as stated previously, the most elusive, has been long chain branching. Long chain branching in high density polyethylenes has long been considered a factor affecting certain observed physical properties, for example, environmental stress cracking, rheological properties and processing behavior although conclusive proof has been difficult to obtain. In low density polyethylenes, the concentration of long chain branches is such (>0.5 per 1,000 carbons) that characterization through size exclusion chromatography in conjunction with either low angle laser light scattering or intrinsic viscosity measurements becomes feasible (9-11)(13)(17-18). When carbon-13 NMR measurments have been compared to results from polymer solution property measurements, good agreement has been obtained between long chain branching from solution properties with the concentration of branches six carbons long and longer (9)(10). Unfortunately, these techniques utilizing solution properties do not possess sufficient sensitivity to detect long chain branching in a range of one in ten thousand carbons, the level suspected in high density polyethylenes. The availability of superconducting magnet systems has made measurements of long chain branching by C-13 NMR a reality because of a greatly improved sensitivity. An enhancement by factors between 20 to 30 over conventional NMR spectrometers has been achieved through a combination of higher field strengths, 20 mm probes, and the ability to examine polymer samples in essentially a melt

state. Th
both conve
of 23.5 kG
Let us no
branching
tivity and
limit.

The C
ethylene 1
with 1-oct
branches a
bons in le
less than
spectral f
chemical s
parameters
ethylene-1
nate those
by C-13 NM

The distin
bols while
starting w
bon bonded
resonance
in Figure
the same a
"4" carbon
likewise,
linear pol
C-13 spect
Carbon-13
linear six
length or

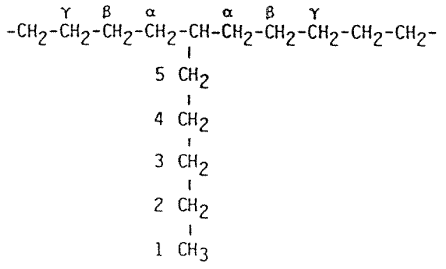
echnique for
ion. Now it
aturated end
equently, an

rately in a
ing ethylene
s the densi-
ommonly used
igh pressure
used to mea-
ently of the
distinct ad-
use the lat-
spective of
a chain end
disadvantage
carbons in
y of longer
h and longer
pendently of
the longer
ver, in the
hain branch-

ent and, as
hain branch-
nes has long
ed physical
ng, rheologi-
lusive proof
hylenes, the
r 1,000 car-
romatography
attering or
-11)(13)(17-
ared to re-
od agreement
om solution
carbons long
es utilizing
sitivity to
ten thousand
ylenes. The
ade measure-
because of a
ctors between
een achieved
mm probes,
ially a melt

state. The data discussed in this study have been obtained from both conventional iron magnet spectrometers with field strengths of 23.5 kG and superconducting magnet systems operating at 47 kG. Let us now begin our discussion of polyethylene long chain branching with an examination of the C-13 NMR structural sensitivity and later turn to quantitative sensitivity and detection limit.

The C-13 NMR spectra from a homologous series of six linear ethylene 1-olefin copolymers beginning with 1-propene and ending with 1-octene are reproduced in Figures 2 and 3. The side-chain branches are, therefore, linear and progress from one to six carbons in length. Also, the respective 1-olefin concentrations are less than 3%; thus, only isolated branches are produced. Unique spectral fingerprints are observed for each branch length. The chemical shifts, which can be predicted with the Grant and Paul parameters (5)(19) are given in Table I for this series of model ethylene-1-olefin copolymers. The nomenclature, used to designate those polymer backbone and side-chain carbons discriminated by C-13 NMR, is as follows:



The distinguishable backbone carbons are designated by Greek symbols while the side-chain carbons are numbered consecutively starting with the methyl group and ending with the methylene carbon bonded to the polymer backbone (5). The identity of each resonance is indicated in Figures 2 and 3. It should be noticed in Figure 3 that the "6" carbon resonance for the hexyl branch is the same as α, the "5" carbon resonance is the same as β, and the "4" carbon resonance is the same as γ. Resonances 1, 2 and 3, likewise, are the same as the end group resonances observed for a linear polyethylene. Thus a six carbon branch produces the same C-13 spectral pattern as any subsequent branch of greater length. Carbon-13 NMR, alone, therefore cannot be used to distinguish a linear six carbon branch from a branch of some intermediate length or a true long chain branch.